ISTANBUL TECHNICAL UNIVERSITY ★ INSTITUTE OF SCIENCE AND TECHNOLOGY

ELECTROCHEMICAL SYNTHESIS AND CHARACTERIZATION OF POLYANILINE THIN FILMS

M.Sc. Thesis by

Dilek ÇAKIROĞLU

(515041012)

Date of submission : 8 May 2006

Date of defence examination: 14 June 2006

Supervisors : Prof.Dr. A. Sezai SARAÇ

Assoc. Prof. Dr. Esma SEZER

Members of the Examining Committee: Assoc. Prof.Dr. Ayfer SARAÇ (Y.T.Ü.)

Assoc. Prof.Dr. B. Filiz ŞENKAL (İ.T.Ü.)

Assoc. Prof.Dr. B. USTAMEHMETOĞLU (İ.T.Ü.)

Prof.Dr. Seniha GÜNER (İ.T.Ü.)

MAY 2006

İSTANBUL TEKNİK ÜNİVERSİTESİ ★ FEN BİLİMLERİ ENSTİTÜSÜ

İNCE POLİANİLİN FİLMLERİN ELEKTOKİMYASAL SENTEZİ VE KARAKTERİZASYONU

YUKSEK LİSANS TEZİ
Dilek ÇAKIROĞLU
(515041012)

Tezin Enstitüye Verildiği Tarih : 8 Mayıs 2006
Tezin Savunulduğu Tarih : 14 Haziran 2006

Tez Danışmanları :	**Prof.Dr. A. Sezai SARAÇ** **Doç.Dr. Esma SEZER**
Diğer Jüri Üyeleri	**Doç.Dr. Ayfer SARAÇ (Y.T.Ü.)**
	Doç.Dr. B.Filiz ŞENKAL (İ.T.Ü.)
	Doç.Dr. Belkıs USTAMEHMETOĞLU (İ.T.Ü.)
	Prof.Dr. Seniha GÜNER (İ.T.Ü.)

MAYIS 2006

ACKNOWLEDGEMENT

First of all, I would like thanks my adviser, Professor Dr. A. Sezai SARAÇ for his guidance, inspiration and encouragement throughout this work, and for the opportunity to work in his research group. I would also like to exppress my sincerest thanks to adviser, Assoc. Professor Esma SEZER for their boundless enthusiam, indispensable advice and encouragement.

I would like to thank Assoc. Professor B.Filiz Şenkal for the synthesis of aniline salt. Also, I would like to acknowledge Elif Altürk PARLAK and Fevzi Çakmak Cebeci sharing their knowledge and experiences with me generously throughout this research.

Finally, I would like to offer the most gratitude to my parents for their patience, understanding, moral support and encouragement during all stages in the preparation of this thesis.

May 2006 Dilek ÇAKIROĞLU

TABLE OF CONTENTS

ABBREVATIONS

ANI	: Aniline
PANI	: Polyaniline
ANIHCI	: Anilinium Hydrochloride salt
PANI-CI	: Polyanilinium Doped with Chloride
PANIHCI-CI	: Polyanilinium Hydrochloride Salt Doped with Chloride
MS	: Methane Sulphonice Acid
ANIMS	: Anilinium Methane Sulphanate salt
PANI-MS	: Polyanilinium Doped with MS
PANIMS-MS	: Polyanilinium Methane Sulphate Salt Doped with Chloride
LB	: Leucoemeraldine
EB	: Emeraldine
PB	: Pernigrenaline
CV	: Cyclic Voltammetry
EIS	: Electrochemical Impedance Spectroscopy
SEM	: Scanning Electron Microscopy
FTIR	: Fourier Transform Infrared
UV	: Ultra Violet
ITO	: Indium-Thin oxide

LIST OF TABLES

LIST OF FIGURES

ELECTROCHEMICAL SYNTHESIS AND CHARACTERIZATION POLYANILINE THIN FILMS

SUMMARY

In 1977, MacDiarmid and his friends discover that when polyacetylene is doped with iodine, its conductivity increase many orders of magnitude. After this discovery, conducting polymers have generated much scientific interest. Polyaniline is a very important material in the class of conducting polymers because it is synthesized easily, it is environmental stabile, it has good redox properties and very large usage field like as microelectronic, corrosion prevention.

Polyaniline (PANI) is synthesized with electrochemical or chemical methods. It has different intrinsic oxidation states, leucoemeraldine (LB), emeraldine (EB) and pernigrenaline (PB). LB and PB form is fully reduced and oxidized form of the polyaniline, respectively. In the EB form, reduced and oxidized units are equal number. Emeraldine salt is the only conducting form of the PANI.

Polymer growth of PANI is affected from the type, size and shape of the dopant, concentration of the dopant, pH of the acid in the same way, conductivity of the PANI depends on the degree of doping, oxidation state, and the particle morphology.

The aim of this study was to obtain the best polymeric films of aniline having good conductivity and supercapacitor properties. Electrochemical coating of polyaniline onto platine electrode was investigated in different electrolytes and different cycle numbers for different aniline derivatives. All of these thin films were characterized by FT-IR, Cyclic Voltammetry (CV), and Electrochemical Impedance Spectroscopy (EIS). These thin films are also characterized in morphology by Scanning Electron Microscopy (SEM). Also, in situ electrochemical study for thin film obtained from aniline monomer doped with methane sulphonic acid (MS) were carried out on an optically transparent electrode (Indium thin oxide (ITO) coated glass) in MS acid. Electrical conductivities of the polymers are measured with four point probe solid conductivity.

Firstly, aniline and aniline chloride salt were electrodeposited on platinum bottom electrode in the HCI acid for 8 and 16 cycles. The same experiment was made for aniline and aniline methane sulphanate salt in the MS acid. The electrochemical behaviors were investigated by cyclic voltammetry. One of the aims in this study is the learning whether aniline monomer or its salt is good choice for obtaining films having good conductivity. Experiments indicate that starting from aniline monomer to obtain thin film gives the best result and increasing film thickness are good for conductivity properties of thin films. Also, results indicate that organic acids provide better media than inorganic acids.

In order to perform solid state conductivity measurements, polymerization reactions were performed electrochemically at a constant potential in the HCI and MS acids containing monomers. Polymeric films were deposited potentiostatically onto platinum plate electrodes. The conductivity measurements were shown very high values as 3 S/cm^{-1} for polyaniline obtained in MS acids.

EIS was employed to monitor capacitor behaviors of films being excited at the peak voltages and 0.0 voltages for 2 seconds. Also, effect of different cycle numbers and different electrolytes were investigated. EIS results confirm that thin films obtained from MS acid have better capacitive properties than films obtained from HCI acid.

Also, with the FT-IR and UV measurement doping level and oxidation state of all polymers are analyzed. This results support the CV result because polymers obtained in MS acid have the highest doping level because of this, this polymer has the highest conductivity. Also, results from UV and FT-IR indicate that obtained polymers are about conducting form. SEM images indicate that PANI films obtained from HCI has homogen surface whereas films obtained from MS has porous and globular surface. These results are agreed with the EIS measurement results.

Finally, in-situ spectroelectrochemical measurement was made for polyaniline film obtained in MS acid. In obtained absorbance vs wavenumber graph, there is a one shoulder at the around 750nm and there is an increase in absorbance with the increasing applied voltage. This is ascribed to formation of the charge carriers in the polymer chains.

İNCE POLİANİLİN FİLMLERİN ELEKTOKİMYASAL OLARAK SENTEZİ VE KARAKTERİZASYONU

ÖZET

1977`de, MacDiarmid ve arkadaşları, polyasetilenin doplanması ile iletkenliğinin arttığını bulmuşlardır. Bu buluştan sonra bilim dünyasında, iletken polimerlere karşı ilgi uyanmıştır. Polianilinin; kolay sentezlenebilmesi, dayanıklılığı, güzel redoks özellikleri ve kullanım alanının genişliği (mikroelektronik, korozyon önleme), onu iletken polimerler arasında en önemlilerden biri haline getirmiştir.

Polianilin (PANI), kimyasal ve elektokimyasal olarak sentezlenir. Leucoemeraldin (LB), emeraldin (EB) ve pernigrenalin (PB) olmak üzere değisik oksidasyon formları vardır. LB ve PB formu sırası ile tamamen indirgenmiş ve tamamen yükseltgenmiş formlarıdır. EB formunda ise indirgenmis ve yükseltgenmiş birimlerin sayısı eşittir ve yalnızca emeraldin tuzu, PANI`nin iletken formudur.

Kullanılan asidin pH`ı, dopantın büyüklüğü, tipi, şekli ve konsentrasyonu, polianilinin oluşmasında önemli rol oynarlar. Aynı şekilde, PANI`nin iletkenliğinide etkileyen; doplanma derecesi, oksidasyon durumu ve polimerin morfolojisi gibi faktörler vardır.

Bu çalışmanın amacı, iyi iletkenlik ve süperkapasitör özelliklere sahip polyanilin filmleri elde etmektir. Anilin ve türevleri, farklı kalınlıkta ve faklı çözelti içinde Platin elektrod üzerine elektrokimyasal olarak kaplanmıştır. Elde edilen filmler, UV görünür bölge, FT-IR ve electrochemical impedance spektroskopi (EIS) yöntemleri ile karakterize edilmiştir. Taramalı electron mikroskobu (SEM) ile de morfolojik özelliklerine bakılmıştır. Ayrıca, aniline monomerinin methan sulfonik asid ile doplanamasından elde edilen ince fimler, ITO cam elektrodlar uzerinde in situ elektokimyasal çalışmaları yapılmıştı. Katı hal iletkenlikleri de ayrıca incelenmiştir.

Anilin ve anilin klorür tuzunun platin elektrod üzerine 0.1 M HCI asidi içinde 8 ve 16 döngü uygulanarak polimerleri elde edilmiştir. Aynı deney anilin ve anilin methan sulfanat tuzu için 0.1 M metan sülfonik asitte (MS) yapılmıştır. Elektrokimyasal davranışlar döngülü voltametri ile incelenmiştir. Polimerik filmlerin fiziksel

özelliklerin anilinin ve anilinin tuzları kullanılarak karşılaştırmalı olarak incelenmesi amaçlanmıştır. Deney sonuçları, ince film eldesine anilin monomerinden başlamanın en iyi sonuçları verdiğini ve film kalınlığının artmasının, ince filmin iletkenlik özellikleri için iyi olduğunu göstermiştir. Ayrıca, sonuçlar, organik asidlerin inorganik asitlerden daha iyi bir ortam sağladığını göstermektedir.

Katı hal iletkenliğini bakmak için polimerizasyon sabit potansiyelde monomer içeren HCI ve MS asid çözeltileri içinde gerçekleştirilmiştir. Polimerik filmler sabit potensiyel altında platin elektrod üzerine toplanmıştır. İletkenlik sonuçları, 3 S/cm^{-1} iletkenlik ile MS asid ile doplanarak elde edilen filmin en yüksek iletkenliğe sahip olduğunu göstermiştir.

Filmlerin kapasitör özelliklerini incelemek üzere EIS ölçümleri filmin pik potansiyellerinde ve 0.0 V' da 2 saniye uyarılması ile yapılmıştır. Ayrıca farklı döngü sayısının ve elektrolitin etkisi de incelenmiştir. EIS ölçümleri, MS asidden elde edilen filmlerin HCI ortasmında elde edilen filmlerden daha iyi kapasitif özelliklere sahip olduğunu göstermektedir.

Polimerlerin doplanma ve oksitlenme seviyesi FT-IR ve UV ölçümleri ile analiz edilmiştir. Sonuçlar, CV den elde edilen sonuçlari desteklemektedir çünkü MS içinde elde edilen filmler en yüksek doplanma seviyesine ve bu nedenle polimer en yüksek iletkenliğe sahiptir. Ayrıca, sonuçlar elde edilen polimerlerin iletken formda olduğunu göstermiştir. SEM görüntüleri, HCI ortamında elde edilen PANI filmlerin homojen bir yüzeye sahip olduğunu, buna karşılık MS ortamında elde edilen filmlerin porlu yüzeye sahip olduğunu göstermiştir. Bu sonuçlar, EIS ölçümleri ile dogruluk göstermektedir.

Optik özellikleri hakkında fikir sahibi olmak üzere, MS asid içinde elde edilmiş filmin in-situ spektroelektrokimyasal ölçümleri yapılmıştır. Elde edilen absorbans-dalgaboyu grafiğinde, 750 nm civarlarında bir omuz gözlenmektedir. Artan potansiyel ile birlikte absorbansda da bir artış oluşmaktadır. Bu sonuç, polimer zincirinde yük taşıyıcılarının oluştuğunu göstermektedir.

1. INTRODUCTION

Until recently plastics are commonly accepted isolators, but now the electrically conducting plastics, so called synthetic metals or conducting polymers (CP), are becoming a part of our daily life. These polymers have highly extended conjugated electron systems in the main chain so they have received attention from the point of view of both fundamental and practical engineering aspects. It is possible to control the morphologic, electronic and optic properties of these materials and this control provide opportunity to use them for various applications [1-5]. The CPs are widely used in electronic and electrochromic equipments, photochemical cells, recharging batteries, catalysts [6-7] Conjugated polymers were developed as active materials in electronic devices due to their excellent electrical characteristics. Nature of the dopants and molecular structure are important parameters for electronic energy states of conducting polymers. Doping is achieved by chemical or electrochemical methods via injection/expulsion of ions or the application of voltage, and thereby it could be possible to control the electrical conductivity can be varied from insulator range to metal ranges [8]. For example, as PANI is oxidized, in the polymer chain cationic radicals are generated and anions known as counter-ions in the solution enter the film to provide neutrality of the film. In the same way, anions are expelled from the film so PANI is reduced.

The first conducting polymer successfully synthesized was polyacetylene, by Shirakawa in 1974. In 1977, polyacetilene was doped with iodine so conductivity of polymer was increased 10^9 times then the conductivity of non-doped polymer. Since then, several conducting polymers have been synthesized and characterized. Polyaniline (PANI), polythiophene, polypyrrole, and polytphneylene have been studied the most. In 1862, firstly, PANI was prepared anodically in a sulfuric acid solution by H. Letheby of the College of London Hospital. Electrical conductivity of all conducting polymers stems from their extended π-conjugated systems. In Table 1, there are the name, the color change when they are doped/undoped and their conductivity [9].

Table 1: Conducting polymers, their colors, and conductivities.

Polymer	Colour (undpoed → doped)	App.Conductivity (S cm^{-1})
Polyacetilene		10^3 -10^5
Poly(3-alkylthiophene)		10^4 - 10^5
Polyphenylenevinylene		10^5
Polypyrole	yellow-green→blue→black	500-7500
Polythiophene	red → blue	10^3
Polyphenylene		10^3
Polyaniline	Yellow → green → blue	10^2 - 10^3

Polyaniline (PANI), one of the important classes of conjugated polymers, received much attention due to its interesting electrochemical, optical properties and environmental stability. PANI can be doped to its conducting form without changing the number of ה-electrons by treating with protonic acids [10–12]. Polyaniline is soluble in organic solvents such as N-methyl-2-pyrrolidione (NMP), or in concentrated acid (e.g., HCI). Because of the rich redox behaviors, PANI is used in rechargeable batteries, metal protection, absorptive coatings, sensors, and electrochromic devices.

There are a lot of methods to characterize polymeric films. The most important techniques are those; film structure, morphology and porosity have been studied by SEM [13-16], electrochromic properties, film thickness, and film density have been characterized by UV-vis spectroscopy [17], film capacitance, transport, and structural information have been examined by electrochemical impedance spectroscopy (EIS) [18-22]. CV technique is important analytical technique used in electrochemistry [23, 24].

In this study, thin films are obtained on the platinum bottom electrode from aniline monomer and its chloride and methane sulphonice salt which doped with HCI and CH_3SO_3H. These thin films were analyzed with CV method. Also, EIS was used to examine supercapacitive properties of films and the structure and morphology of the PANI films were investigated through the measurements of Scanning Electron Micrograph (SEM), FT-IR and UV-visible. In-situ measurement are made for PANI-MS films on ITO glass electrode.

2. THEORETICAL PART

2.1. Conducting Polymers

Conducting polymers (CP) are commonly known as “synthetic metals” and these polymers possess not only mechanical properties and processibility of conventional polymers, but also unique electrical, electronic, magnetic and optical properties of metals, which conventional polymers do not have [25]. Conducting polymers are conjugated polymers, namely organic compounds that have an extended pi-orbital system, through which electrons can move from one end of the polymer to the other. The commonly studied organic polymers are polyacetylene, polypyrrole, polyaniline, and these polymer`s derivatives. All these polymers (Figure 2.1.) have one characteristic future, which is they all have highly conjugated backbone.

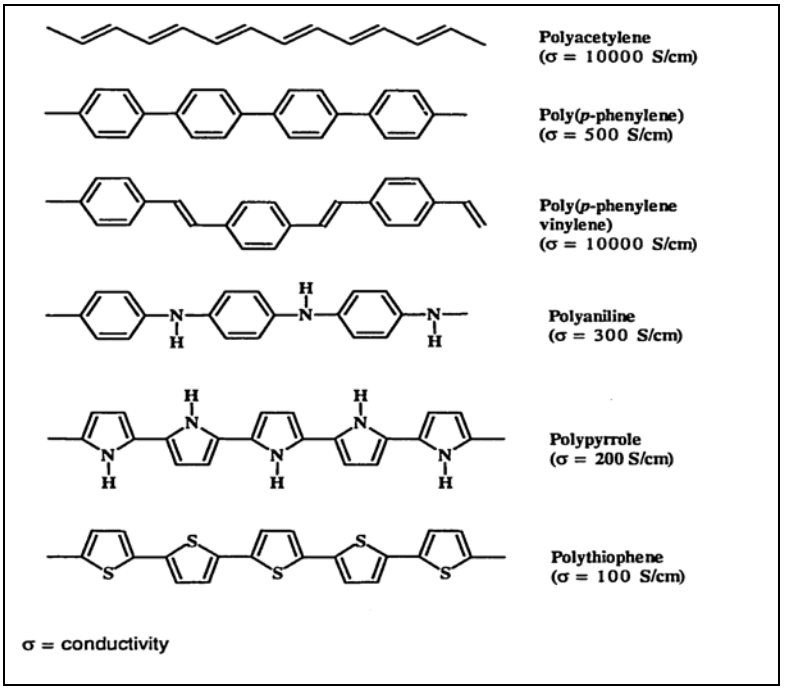

Figure 2.1: Some conducting polymer structures.

The conductivities of the pristine (undoped) electronic polymers are transformed from insulating to conducting through the process of doping. Conductivity increases with the increasing doping level. The concept of doping is striking theme which

distinguishes conducting polymers from all other types of polymers. Doping process is made with using dopant molecule. There is a wide variety of dopant ions , the nature of the dopant ions associated with the polymer are precisely known. These materials are generally doped with protonic acids such as aqueous hydrochloric acid (HCI) to give conductivity of the order of 1 S/cm^2 [26-28] Electronic, electrical, magnetic, optical and structural properties of the polymer are changed by the controlled addition of small quantities of chemical species.

2.1.1 The Concept of Doping

The concept of doping is understood very well because this concept distinguishes CP from other types of polymers. CP can have two different forms; conductive form (doped form) and non-conductive form (non-doped polymer). All conducting organic polymers are insulators or semiconductors in their neutral forms [25]. In doping process, polymer is converted from neutral forms to charged or conducting forms. The electrical conductivity of a doped material is 5-10 orders of magnitude higher than that of the non-doped material. Doping and dedoping are reversible processes which do not change the chemical nature of the original polymer backbone.

2.1.2 Polaron and Bipolaron Theory

CP may be doped electrochemically or chemically. Electrical conduction mechanism in polymers is explained with polaron / bipolaron theory. Electrochemical doping is done by applying an external reductive (n-doping) or oxidative (p-doping). When the polymer are oxidized by an external oxidizer termed dopant, charge carriers called polarons are created along the polymer backbone. A polaron (.+) or radical cation is achieved by electron transfer from a conjugated polymer to an oxidant (dopant), unpaired electron coupled with a positive charge is the direct result of this transfer. At high doping level, the unpaired electron in the polaron structure is removed resulting in the formation of bipolaron (Figure 2.2). Bipolaron has a charge of +2e.

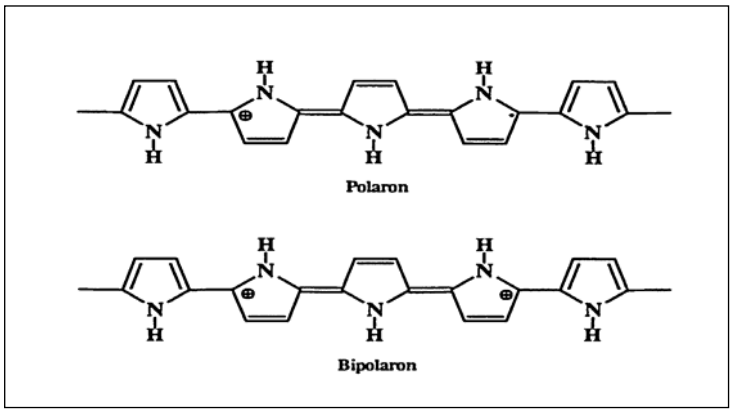

Figure 2.2: Polaronic/Bipolaronic Polypyrrole

After the doping mechanism, the charge carrier can be delocalized along the backbone chain so a conducting polymer is achieved. If the radical cation can overcome the columbic binding energy to the acceptor anion with thermal activation energy or at high dopant concentrations, the polaron will move or delocalize throughout the backbone and contribute to the electrical conductivity [29]. The dopant concentrations required for maximum conductivity are exceptionally high, typically accounting for 50% of the final weight of the conducting polymer [30].

2.2. Polyaniline

Polyaniline (PANI) is a typical phenylene-based polymer having a chemically flexible –NH- group in a polymer chain flanked either side by a phenylene ring. The protonation, deprotonation and various other physicochemical properties of polyaniline can be said to be due to the presence of the NH group [31].

(PANI) is unique among the family of conjugated polymers because its doping level can be controlled with acid doping/base dedoping process. PANI has high conductivity, good redox reversibility, environmental stability [32]. It is insoluble in most common organic solvents, and has proton exchange and redox properties [33]. Furthermore, it is easily synthesized and shows simple non-redox doping by protonic acids. In non-redox doping, number of electrons in polymer chain is the same during the all polymerization time because nitrogen atom is protonated. This protonated form is electronically conducting, and conductiviy is a function of level of protonation as well as functionalities present in the dopant [31].

Several researches show that some of the oxidized form of PANI and its derivatives obtained by electrochemical oxidation of aniline has a lot of application field such as energy storage devices, electrochemical-chemical sensors, electrochromic devices and corrosion protection [34 -41]. Good results have been obtained with functionalized PANI in gas sensors and the proposition of PANI doped with 2,5-dimercapto-1,3,4-thiadiazole (DMcT) as an alternative material for high-energy cathodes in lithium batteries [42-44].

2.2.1 Electrochemical Synthesis of Polyaniline

Polyaniline can be synthesized by chemical or electrochemical oxidation of aniline under aqueous acidic conditions by applying an appropriate anodic potential or a potential cycling procedure. One of the most useful methods for the preparation of PANI and its ring substituted derivatives is electrochemical synthesis [45]. Electrochemical synthesis is usually carried out by CV with the cathodic potential in the range between –0.2V and 0V vs. SCE and the anodic potential in the range between 0.7V and 1.2V vs. SCE in acidic aqueous solutions containing monomer [46, 47].

Experimental parameters of the synthesis and method of the preparation affect the PANI deposation. Zotti, who investigated the mechanism and growth of polyaniline by CV, found that polyaniline growth depends greatly on the type and concentration of the supporting electrolyte anion [48]. The effect of dopant dimension on PANI film structure was studied by scanning microscopy [49]. By analyzing the microstructure of PANI films doped with perchlorate, p-toluene sulphonate, and camphor sulphonate counteranions, they found that the distance between PANI molecular chains depends on the size and the geometry of the dopants. This implies that the structure of the doped PANI film is influenced by the dimension and geometric shape of the dopants. The importance of the molecular size of the dopant was mentioned by Trivedi [50]. Furthermore, thickness and electrolyte pH is strongly affected by the nature of the anion of the acid used as electrolyte during PANI growth [51,52]. For example, PANI has only low conductivity and a little electrochemical activity at pH>4 and its usable potential range also decreases with increasing pH value [53].

Electrochemical synthesis is achieved by using; galvanostatic, potentiostatic and sweeping the potential methods. CV is selected to obtain PANI film with lower background current and better electrochemical characteristics [54].

The electrical conductivity is the most important property of PANI and impedance measurements were used for conductivity studies as well as to elucidate mechanism and kinetics of chemical and electrochemical reactions at PANI films [55-66] and substituted PANI derivatives [67–71], deposited as thin films on different electron conducting substrates.

2.2.2 Conductivity of PANI

The chemistry of PANI is more complex than that of other conducting polymers. PANI has a very of oxidation states that are both pH and potential dependent [72] and these forms differ in chemical and physical properties [73-75]. The most well known base form of PANI is that leucoemeraldine (LEB, fully reduced), emeraldine (EB, half-oxidised) and pernigraniline (PNB, fully oxidised) [76]. In Figure 2.3, there are structures of conducting and insulating form of PANI.

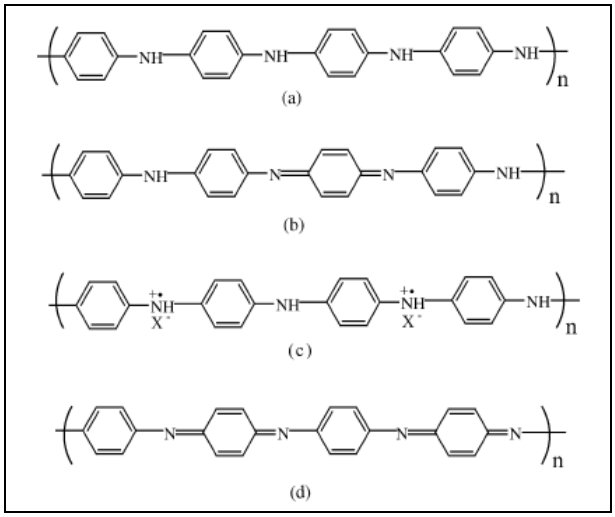

Figure 2.3: Four different forms of PANI: (a) leucoemeraldine base, (b) emeraldie base, (c) conducting emeraldine salt (half-oxidized and protonated form), (d) pernigraniline base.

These forms can be generalized like as depicted in the Figure 2.4, (1-y) can vary from 0 to 1 and shows the fraction of oxidized units (containing imine species, –N=). When (1-y) is zero, polymer has only reduced unit (containing amine species, -N-), this form is known as leucoemeraldine base and PANI is an insulator in this form. When (1-y) is 1, polymer is pernigrenaline base, and its energy gap is about 1.4 eV.

When (1-y) is 0.5, that is number of reduced and oxidized units are equal, this form is known as emeraldine base, and its energy gap is about 3.6V which is similar to leucoemeraldine [77].

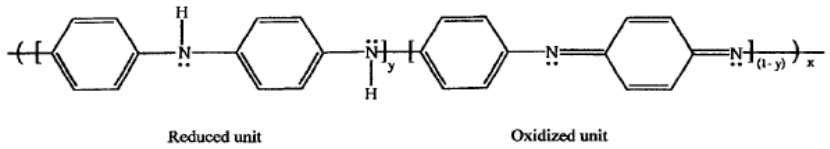

Figure 2.4: Conductivity structures of PANI

According to the authors, ‘‘the slowest step in the polymerization of aniline is the oxidation of aniline monomer to form dimeric species (i.e. p-aminodiphenylamine, PADPA,N-N9-diphenylhydrazineand benzidine), because the oxidation potential of aniline is higher than those of dimers, subsequently formed oligomers and polymer. Upon formation, the dimers are immediately oxidized and then react with an aniline monomer via an electrophilic aromatic substitution, followed by further oxidation and deprotonation to afford the trimers. This process is repeated, leading eventually to the formation of PANI. Wei suggested polymerization mechanism for PANI like as in figure 2.5 [75].

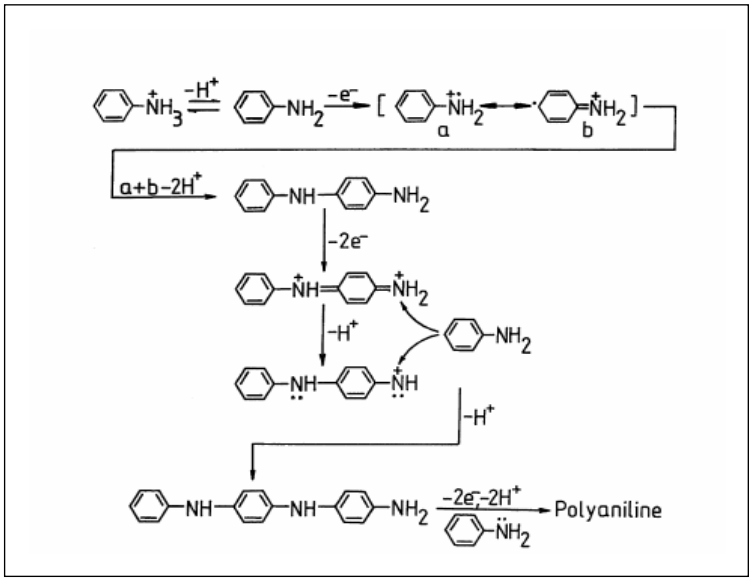

Figure 2.5: Polymerization mechanism of aniline.

Different oxidation states of PANI have different colors; luecoemeraldine is pale yellow, emeraldine is green, pernigreaniline is violet [78, 17].

The emeraldine base form of PANI can be converted from an insulating (conductivity $\sigma \sim 10^{-10}$ S cm^{-1}) to a `metallic` state ($\sigma \sim 4 \times 10^{2}$ S cm^{-1}) [79]. The emeraldine form of PANI has the highest conductivity because of the extensive π conjugation in the polymer chains. The conductivity PANI depends on two variables:

(i) the degree of oxidation of PANI

(ii) the degree of protonation of the material.

The conducting emeraldine salt (ES) form of PANI is achieved upon protonation of the EB by exposure to protonic acids or oxidative doping of the LB [103]. Also, protonated PANI, (e.g., PANI hydrochloride) converts to a nonconducting blue emeraldine base when treated with ammonium hydroxide (Figure 2.6.) [17].

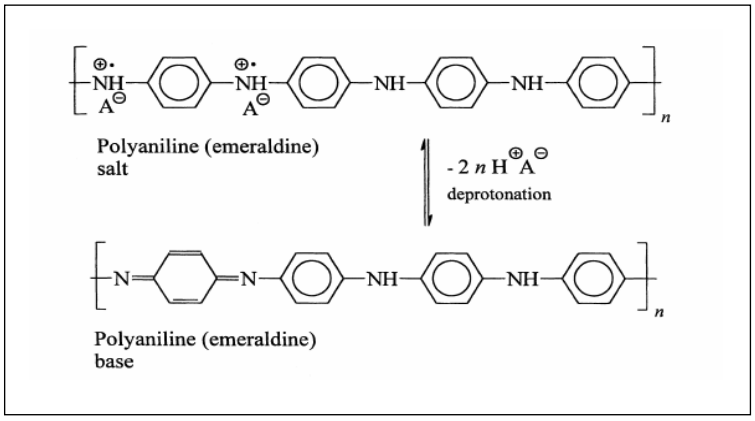

Figure 2.6: Polyaniline (emeraldine) salt is deprotonated in the alkaline medium to polyaniline (emeraldine) base. A– is an arbitrary anion, e.g., chloride.

2.2.3. Redox properties of PANI

PANI undergoes reversible redox reactions. Some proposal was made redox behavior of the PANI, which took into consideration the effect of protonation and counter-anion insertion. The nature of these processes depends on the solution of pH, type of solution anion present, the aniline concentration, the potential and the direction of potential scan [80-82].

Figure 2.7 shows the polymer growth of the aniline on the Pt electrode. In the first CV cycle, the anodic peak appearing at 1.1 V is attributed to the oxidation of PANI monomers and is due to the generation of free radical [31].

In subsequent cycles voltammograms assume shapes giving the number of peaks in both forward and reverse scans. The magnitude of first peak is a measure of the amount of polymer formed [83, 84].

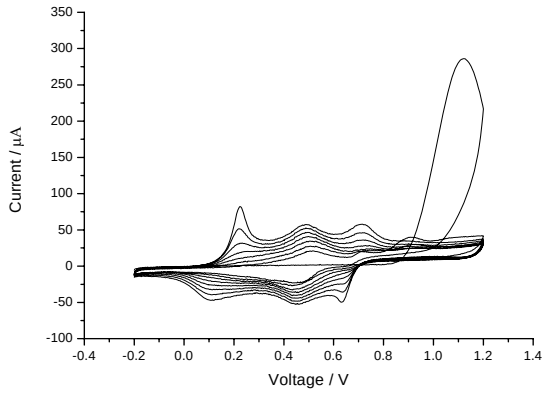

Figure 2.7: Polymer growth of ANI on Pt electrode in 0.5M HCI solution containing 0.1M aniline for 8 cycles; scan rate= 100mV/s.

In CV experiments, characterization of PANI film in the monomer free solution usually gives three anodic peaks. Figure 2.8 shows the voltammetric result for single complete sweep. The sweep rate is 30mV/s. Peak a–a` corresponds to the PANI first redox oxidation-reduction process leading to the formation of cation-radicals. Peak b is attributed to the quinoine/hydroquinone couple forming during the polymerization of aniline and absorbed into the polymer matrix and adsorbed on the electrode surface as suggested elsewhere [84]. Peak c–c` corresponds to the second PANI redox process leading to the formation of dication-diradical. Reaching the potential of peak c is necessary for the polymerization reaction to propagate [85].

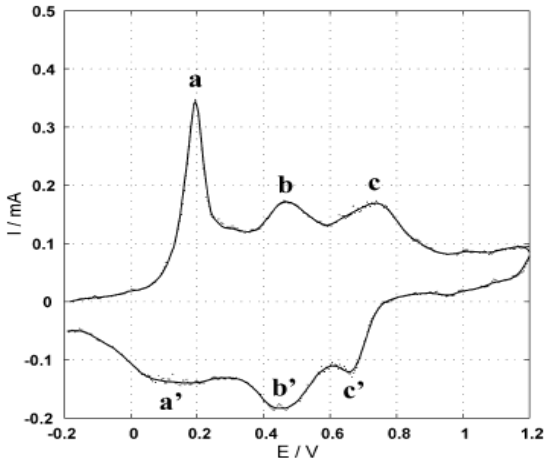

Figure 2.8: Voltammetric curve for 30mV/s sweep rate.

Two scientist, Glarum and Stilwell suggested mechanism to explain peaks in the CV as seen in the figure 2.9 [31].

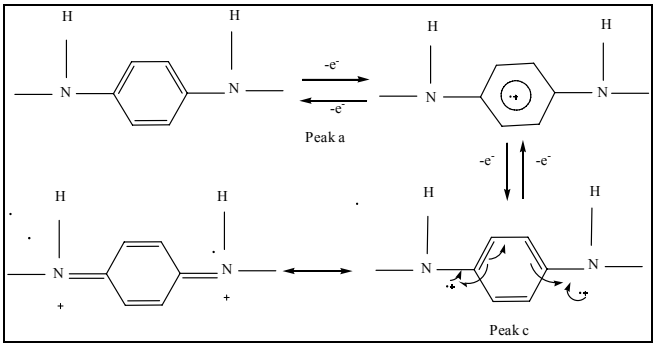

Figure 2.9: Formation of radical cation and diradical-dication.

Polymerization is a self-catalysing reaction and obeys the law $i/nFA=K_c$, where K_c is the autocatalytic rate constant and has a value of approximately $0.47s^{-1}$ for a film of 140 nm [31].

The first step in the oxidation of aniline is the formation of radical cation, which is the independent of the pH. The reaction can be written as figure 2.10 [31].

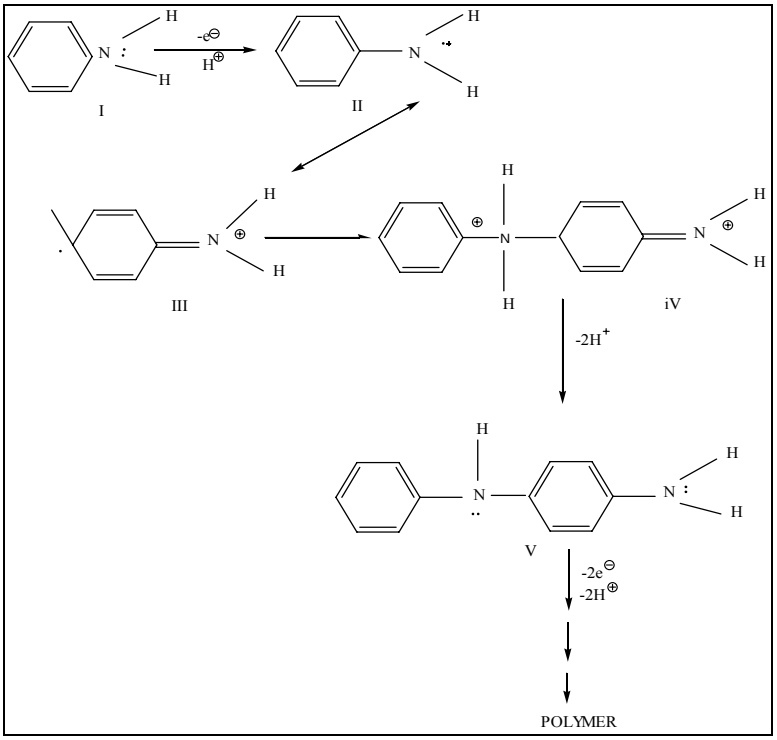

Figure 2.10: Formation of polymer

This radical cation is resonance stabilized and can be represented by the canonical forms shown in figure 2.11.

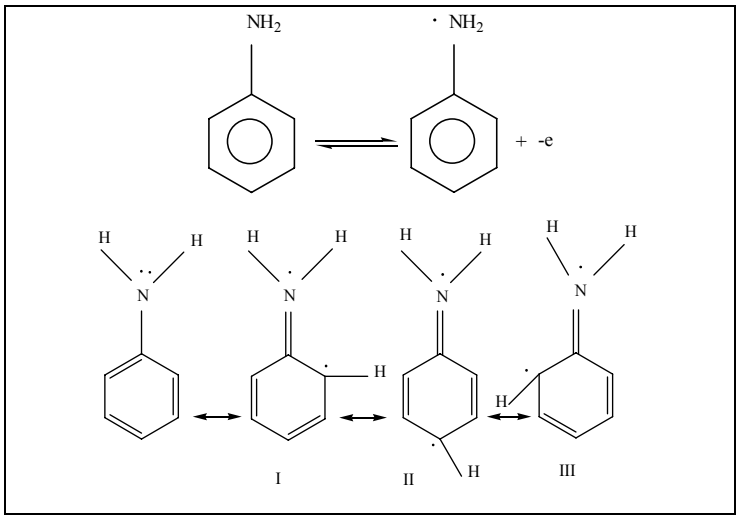

Figure 2.11: Resonance forms of aniline.

The intermediate peaks have been associated to the degradation of PANI salts [86, 87]. The radicals can degrade to give such degradation products such as p benzoquinone, hyroquinone, p-aminophenol, and quinoneimine [88, 89]. This degradation mechanism as proposed by Kobyashi e al. [31] is given in figure 2.12.

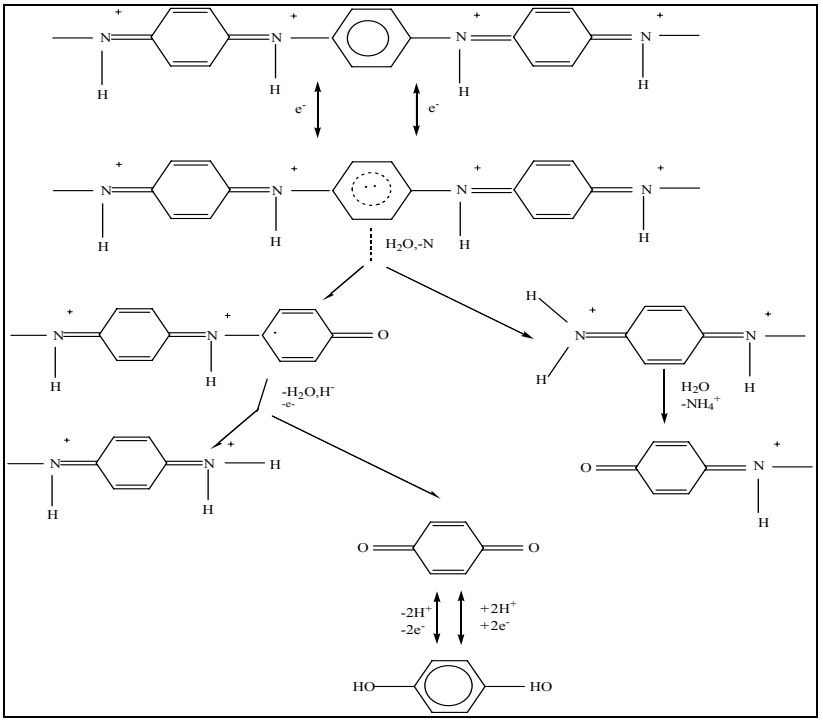

Figure 2.12: The electrochemical degradation of PANI

The presence of degradation product diminishes the electroactivity of the polymer film and its adhesion to the electrode surface [89].

2.3. Electrochemical Impedance Spectroscopy

Impedance measurements are most useful for studying complex systems such as anodic behaviors of metals and other composite materials (90–92), corrosion (93), states of electrodes during charging/discharging cycles of batteries (94-96), surface characterization of polymer-modified electrodes (97-99), and many other complex electrochemical phenomena. Also, it provides a lot of information about the electrochemical characteristics of the subject being examined, like the double layer capacitance, charge transfer resistance, diffusion impedance and solution resistance [100, 101].

2.3.1. Impedance Definition

Ohm's law (Equation 1) defines resistance in terms of the ratio between voltage E and current I.

$$R = \frac{V}{I} \tag{2.1}$$

This well known relationship is limited to only one circuit element. But, the real world contains circuit elements that exhibit much more complex behavior. We use impedance instead of resistance factor. Like resistance, impedance is a measure of the ability of a circuit to resist the flow of electrical current. Electrochemical impedance is usually measured by applying an AC potential to an electrochemical cell and measuring the current through the cell. Assume that we apply a sinusoidal potential excitation; the response to this potential is an AC current signal. This current signal can be analyzed as a sum of sinusoidal functions (a Fourier series).

Electrochemical Impedance is normally measured used a small excitation signal as seen in figure 2.13. There is a phase shift between voltage and current.

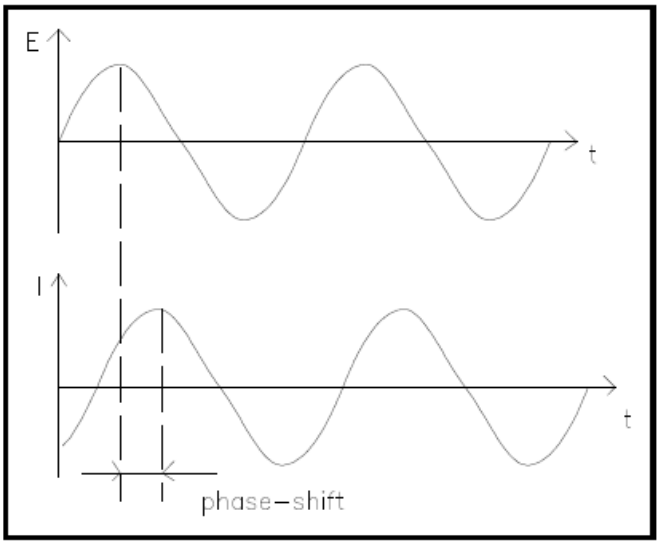

Figure 2.13: Phase shift voltage and current

Excitation signal, Et is the function of the time and expressed as following;

$$Et = E \sin(\omega t) \tag{2.2}$$

ω is the radial frequency (expressed as rad/sec), and has a relationship f (Hertz), frequency, like as

$$\omega = 2\pi f \tag{2.3}$$

In a linear system, the response signal, It, is shifted in phase (ϕ) and has a different amplitude, I_o.

$$I = I \sin(\omega t + \phi) \tag{2.4}$$

An expression analogous to Ohm's Law allows us to calculate the impedance of the system as;

$$Z = \frac{E_t}{I_t} = \frac{E_o \sin(\omega t)}{I_o \sin(\omega t + \phi)} = Z_o \frac{\sin(\omega t)}{\sin(\omega t + \phi)} \tag{2.5}$$

The impedance is therefore expressed in terms of a magnitude, Zo, and a phase shift, ϕ. With Eulers relationship,

$$\exp(j\phi) = \cos\phi + j \sin\phi \tag{2.6}$$

It is possible to express the impedance as a complex function. The potential is described as,

$$E_t = E_o \exp(j\omega t) \tag{2.7}$$

and the current response as,

$$I_t = I_o \exp(j\omega t - \phi) \tag{2.8}$$

The impedance is then represented as a complex number [102],

$$Z(\omega) = \frac{E}{I} = Z_o \exp(j\phi) = Z_o(\cos\phi + j\sin\phi) \tag{2.9}$$

2.3.2. Data Presentation

EIS measurement provides a lot of plot like as Nyquist plot, Bode plot, Warburg plots. Researches can analyze their data with respect to these plots. The Nyquist impedance spectrum consists of a semicircle at high frequencies followed by a linear spike at low frequencies as seen in the figure 2.14. The diameter of the semicircle has been considered as the charge-transfer resistance (R_{ct}) and the high frequency intercept is due to the solution resistance (R_s). An increase in R_{ct} with the thickness of PANI has been reported [103, 104]. Also, the value of Rct increases with the applied voltage [104].

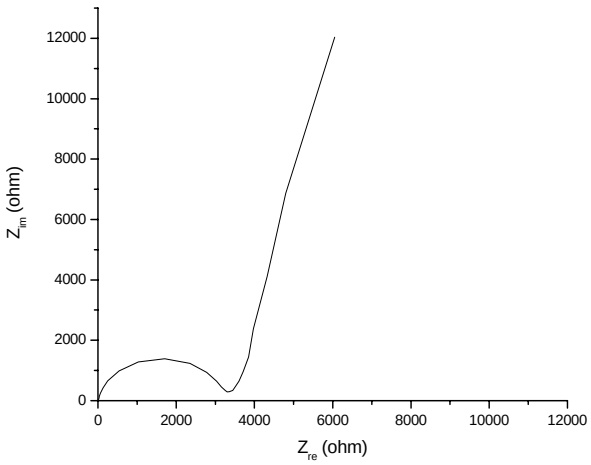

Figure 2.14: Nyquist impedance spectra of PANI/Pt electrodes in 1M CH_3SO_3 at 0.8V vs. Ag/AgCI. Rs=0.0 Ω, Rct=3354 Ω.

In the same way, we can reach some important data from the bode plot. There are several version of the Bode plots like as, Z_{im}-f plot, IZI-f plot, phase of Z (degree)-f plot. Bode phase diagram of figure 2.4 is seen in the figure 2.15.

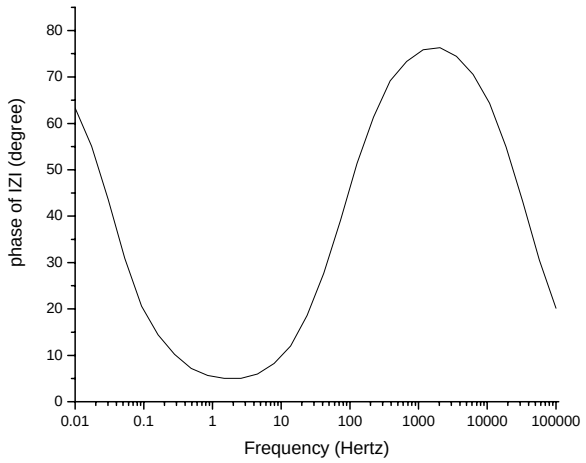

Figure 2.15: Bode phase graphics of PANI/Pt electrodes in 1M CH_3SO_3 at 0.8V.

In this figure, the phase angle is about $63^{0.}$ For a pure capacitor, ϕ is 90^{o} [104]. Figure 2.16 shows plot of the magnitude of Z vs. log w. At intermediate frequencies, the break point of this curve should be a straight line with a slope of -1. Extrapolating this line to the log Z axis at $w = 1$ ($\log w = 0$) yields the value of C_{dl} from the relationship [105];

$$IZI=1/Cdl \qquad (2.10)$$

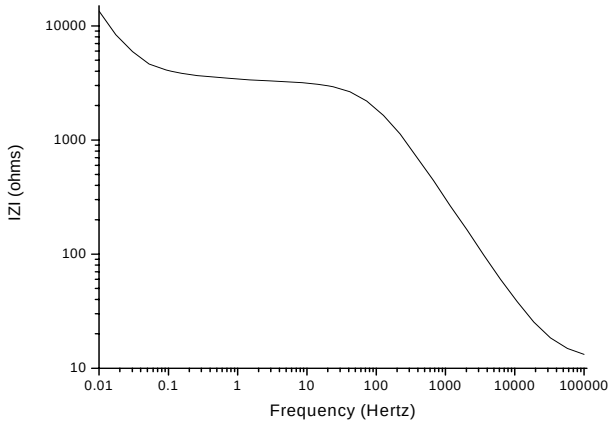

Figure 2.16: The magnitude of Z vs. log w.

We can obtain information about time constant (τ) from the frequency corresponding to the maximum of the imaginary component of the semi circle (figure 2.17), the time constant is calculated using the expression [103, 106];

$$\tau = 1/2\pi f \qquad (2.11)$$

Low values of τ are preferred for electrochemical capacitors in order to ensure charge/discharge characteristics [103, 104, 106].

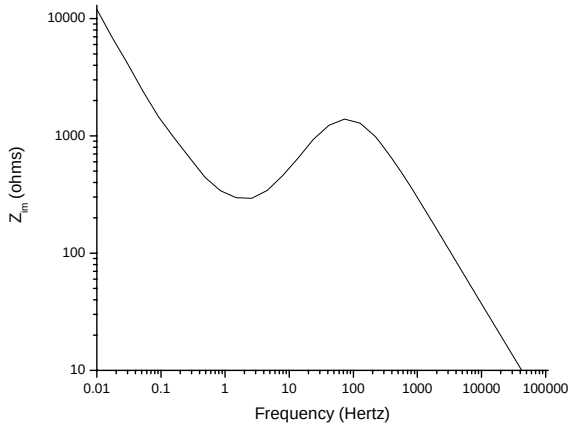

Figure 2.17: The graphs of imaginary part of Z vs. log w.

Furthermore, the low frequency differential capacitance (C_t) is calculated from the variation of the imaginary component of the impedance with the reciprocal of the frequency ($-Z_{im}$ versus 1/f plot) (figure 2.18). The slope is equal to $1/ (2\pi C_t)$ [103, 104].

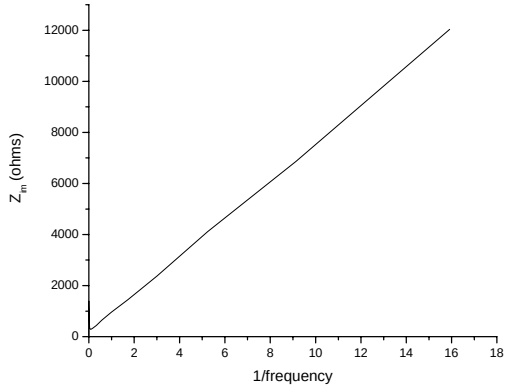

Figure 2.18: The graphs of imaginary part of Z vs. reciprocal of frequency.

3. EXPERIMENTAL WORK

3.1. Electrochemical Equipment

All electrochemical experiments were performed in a 3-electrode cell. For electropolymerization, CV and EIS measurements a PARSTAT 2263 Potentiostat was used. Polymers were analyzed by FT-IR reflectance spectrophotometer (Perkin Elmer, Spectrum One; with a Universal ATR attachment with a diomand and ZnSe crystal C790951) and UV-visible recording spectrophotometer (UV-160A Shihadzu).The morphological studies were analyzed using JEOL JSM-T330 Scanning Electron Microscopy.

3.2. Chemicals

Aniline monomer was provided from Sigma-Aldrich and vacuum distilled before used. Anilinium chloride and methane sulphanate salts were synthesized in our labs. HCI (Sigma-Aldrich) and CH_3SO_3H (Fluka) used as supporting electrolyte. All chemical were analytical grade and no further purification was employed.

3.3. Electrochemical Polymerization Procedure

The electropolymerization reactions were carried out in 0.5M HCI and 1M CH_3SO_3H by the CV technique. The potential was linearly swept between -0.2V and 1.2 V applying 8 cycles and 16 cycles for scan rate of 100 mV/s. Aniline concentrations was 0.1 M in the 0.2 and 1.0 V with six different scan rates, 50mV/s, 100mV/s, 200mV/s, 300mV/s, 500mV/s, 1000mV/s in the monomer free solution for each polymeric film. Impedance spectra were recorded at various electrode potentials E in the reduced and conducting state of PANI. The frequency range was 100kHz to 10mHz. Before each frequency sweep the electrode was prepolarized at E for 2 seconds.

4. RESULTS AND DISCUSSION

4.1. Cyclic Voltammogram of Anilinium and Anilinium Chloride Salt

The polymer growth of anilinium (ANI) and anilinium chloride salt (ANIHCl) were prepared potentiodynamicaly at 100mV/s scan rate applying 8 and 16 cycling on Pt-disc from solutions containing 0.1 M of monomer and 0.5 M HCI as shown in the figure 4.1 and 4.2, respectively (for 16 cycles see figure A.1, A.2, A.3, A.4) and the electrochemical behavior of the these polymer films in 0.5M HCI monomer free solution at different scan rates is shown in inset of figure 4.1 and 4.2.

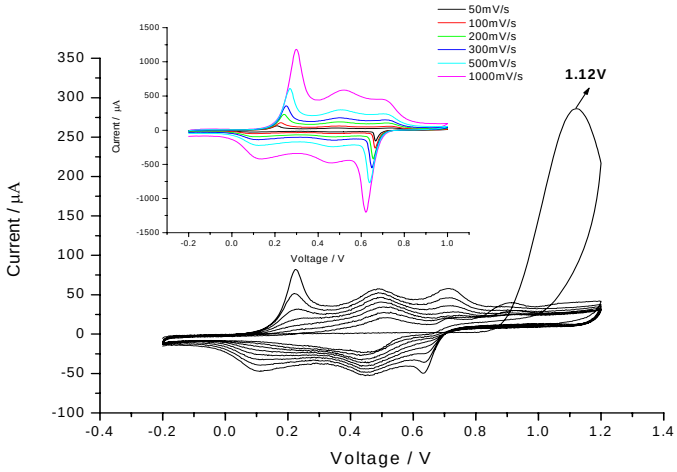

Figure 4.1: The polymer growth of ANI-CI in 0.5M HCI at 100 mV/s scan rate applying 8 cycles. Inset: Scan rate dependence of PANI-CI film in monomer free electrolyte at the different scan rates.

For each PANI type, first radical formation is seen at about 1.12 V and the oxidation and reduction peaks of the film increase as the film grows. There are three oxidation and reduction peaks observed during the growth of the film. The first peak at the ~0.2V belongs to the formation of the leucoemeraldine form to the emeraldine form. The middle peak at the ~0.5V belongs to the degradation or side product of the PANI and third peak at the ~0.75V is the formation of the emeraldine form to the pernigrenaline form.

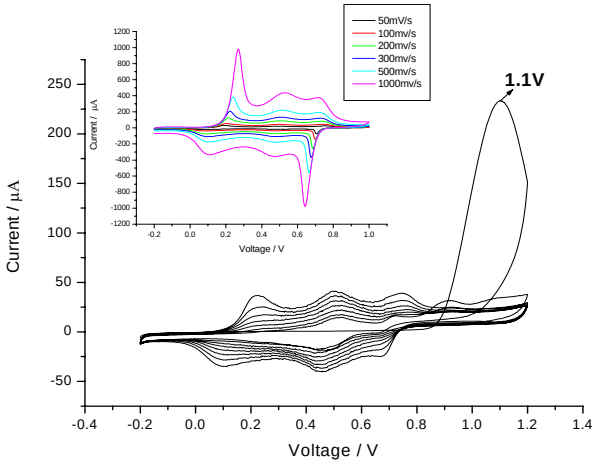

Figure 4.2: The polymer growth of ANIHCI in 0.5M HCI at 100 mV/s scan rate applying 8 cycles. Inset: Scan rate dependence of PANI chloride salt in monomer free electrolyte at the different scan rates.

Degradation peak or middle peak is not observed with the increasing film thickness, and CV studies show that our films are stable because peaks are observed even at the 1000 mV/s scan rate. Furthermore, the CV of PANI grown applying 16 cycles (Figure A.2, A.3) has two peaks, that is, middle peak is not observed with increasing film thickness.

Figure 4.3a shows the comparison of CV of ANI-CI film and ANIHCI-Cl film at the 100mV/s scan rate during and after polymerization. Polymer growths of two polymers are identical in shape in Figure 4.3a, but all peak currents for PANIHCI-Cl are smaller than those for PANI-CI.

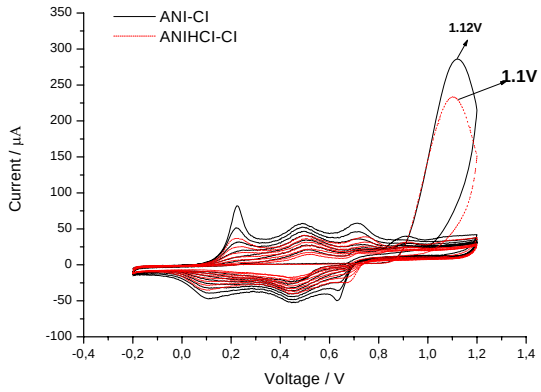

Figure 4.3a: The comparison of CV of ANI-CI and ANIHCI-Cl applying 8 cycles at the 100mV/s scan rate.

It is well known that the plot of I-E on the cyclic voltammogram is equivalent to that of current versus time. That is, the area of the cyclic voltammogram represents the quantity of electricity. As seen in the Figure 4.3 b, the area of PANI-CI is greater than PANIHCI-Cl. Also, there is a positive shift in the first redox potential in the CV of PANI-CI, the reason is that the quinoid unit is more electron-withdrawing unit than the benzenoid unit in polymer chain. In other words, PANI-CI has greater quinoid unit than PANIHCI-Cl.

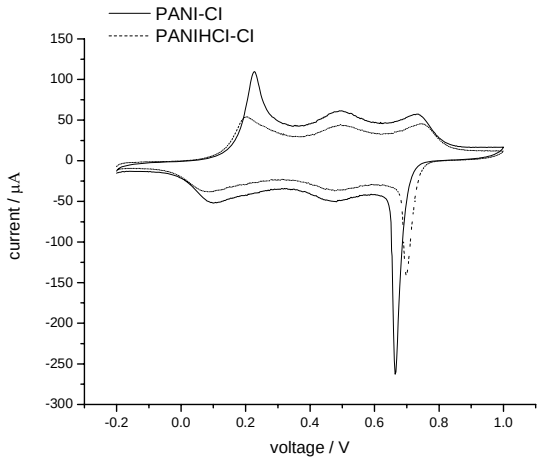

Figure 4.3b: The comparison of CV of PANI-CI and PANIHCI-CI (grown applying 8 cycles) at the 100mV/s scan rate.

This comparison can be made for PANI having different thickness (Figure A.5). With the increasing film thickness, there is no change in the voltage, but current increases. It can be made this explanation for each type of PANI that given in Table 4.1 and 4.2.

Table 4.1: The redox potentials and current values of PANI samples obtained applying 8 cycles in 0.5M HCI

Polymer	E_{a1}/V	I_{a1}/µA	E_{a2}/V	I_{a2}/µA	E_{a3}/V	I_{a3}/µA
PANI-CI	0.22	108.07	0.49	60.91	0.73	56.6
PANIHCI-CI	0.2	53.29	0.49	20.56	0.75	30.36

Table 4.2: The redox potentials and current values of PANI samples obtained applying 16 cycles in 0.5M HCI

Polymer	E_{a1}/V	I_{a1}/µA	E_{a2}/V	I_{a2}/µA	E_{a3}/V	I_{a3}/µA
PANI-CI	0.25	180.39	0.5	52.03	0.73	74.38
PANIHCI-CI	0.22	53.36	0.49	43.55	0.75	44.91

The square root of scan rates for PANI-CI and PANIHCI-CI dependence ($\upsilon^{1/2}$) on the anodic peak current is plotted in figure 4.3c. Peak currents are directly proportional $\upsilon^{1/2}$ and two straight lines are obtained. This means that the electrode reaction rate of PANI films is controlled by mass transfer in the above scan potential rate range.

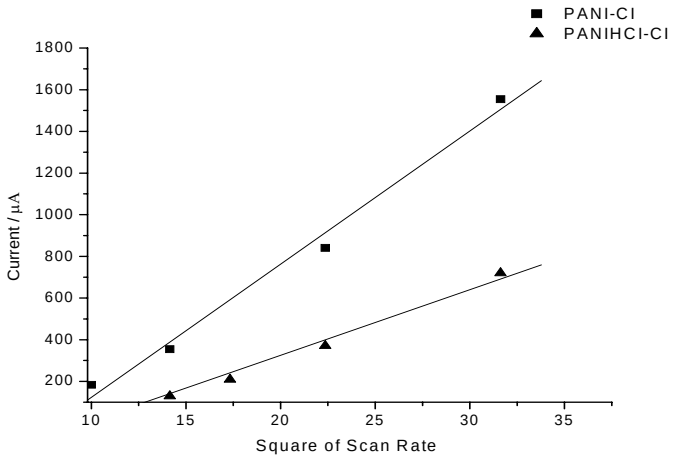

Figure 4.3c: $I_p \sim \upsilon^{1/2}$ plot for the change in the anodic peak current with the scan rate around 0.2V.

4.2. Characterization of PANI-CI and PANIHCI-CI with FT-IR spectra

Figure 4.4 and figure 4.5 shows the IR spectra of PANI-Cl and PANIHCl-Cl. In the PANIHCI-CI, peaks shifted. The ~1270-1280 cm^{-1} and ~776-774 cm^{-1} bands can be assigned to C-N stretching of the secondary aromatic amine and an aromatic C-H out-of-plane vibration, respectively. The characteristic band at ~ 1530-1550 cm^{-1} arises mainly from both C=N and C=C stretching of the quinoid diamine unit, while the band near ~ 1400-1450 cm^{-1} is attributed to the C-C aromatic ring stretching of the benzenoid diamine unit. Intensity ratio (R) of these two peaks indicates the oxidation level of the polymer. A value of 1.0 defines that the emeraldine structure and the polymer can have higher conductivity [87].

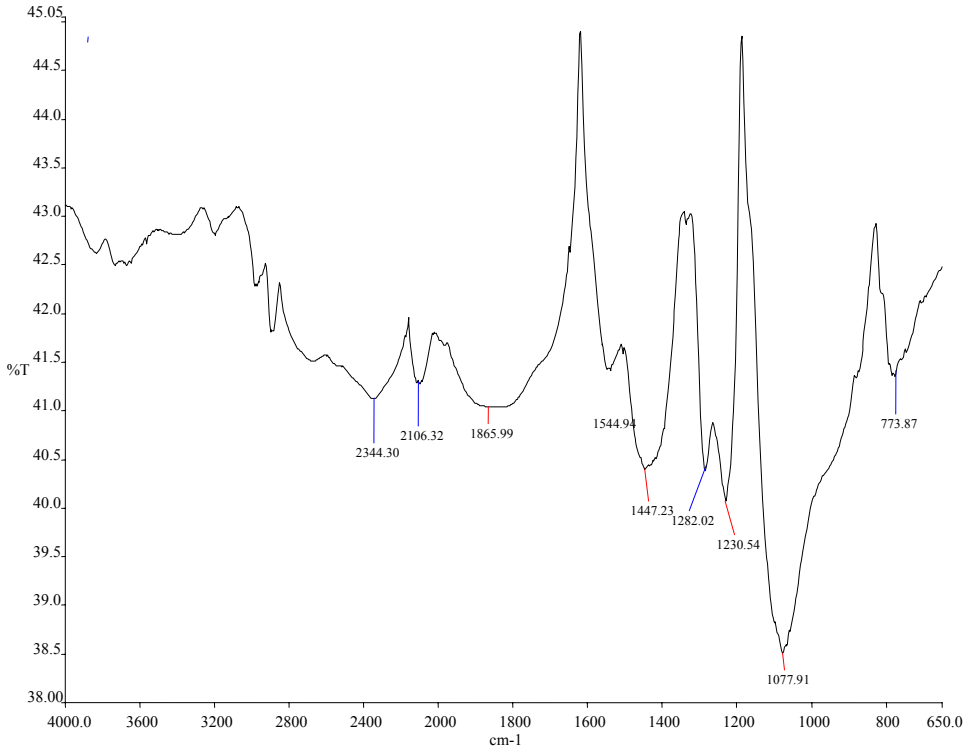

Figure 4.4: FT-IR spectra of PANI-CI

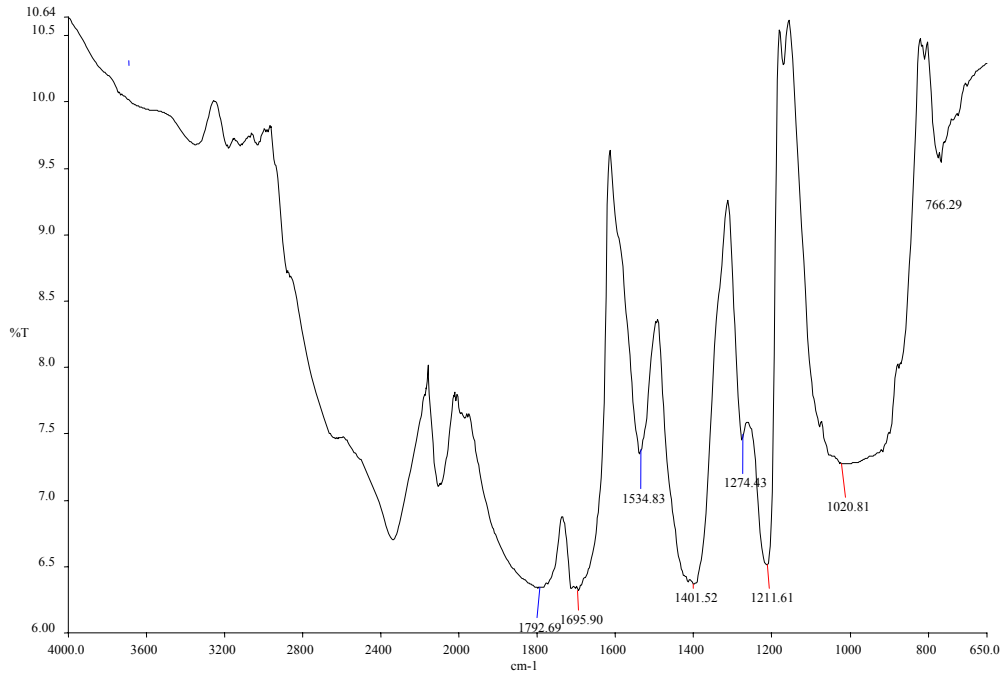

Figure 4.5: FT-IR spectra of PANIHCI-Cl

The peak intensity values calculated from the FT-IR data are listed in Table 4.3. From below results, it can be concluded that the formation of emeraldine form is more predominant in PANI-CI than PANIHCI-Cl.

Table 4.3: The absorption intensity of quinoid and benzenoid units in PANI samples.

Sample	$I_{1530-1550}$	$I_{1400-1450}$	R
PANI-CI	7.37	6.36	1.16
PANIHCI-Cl	41.44	40.41	1.03

4.3. Characterization of PANI-CI and PANIHCI-Cl with UV-visible Absorption Spectra.

PANI-CI and PANIHCI-Cl were dissolved in NMP in the presence of the ammonia and UV measurements are made for these solutions.Then, hydrochloric acid was added to these solutions, UV measurements are made again. Figure 4.6 shows the UV-visible spectra of these PANI films. Figure A.6 and A.7 shows the absorbance level in the basic and acidic medium for these polymers.

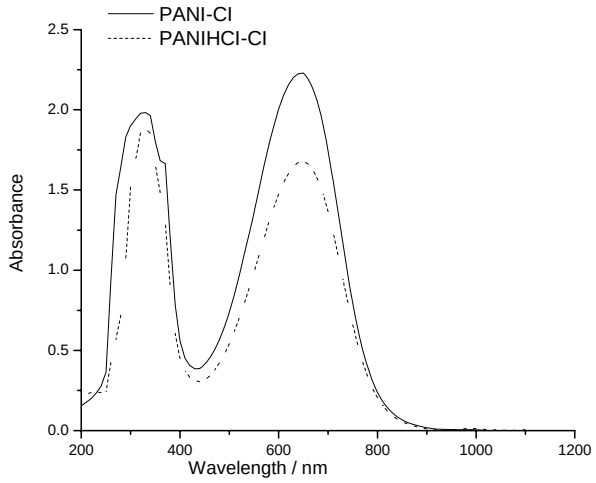

Figure 4.6: UV-visible spectra of PANI samples in the basic medium.

PANI-CI and PANIHCI-CI show two characteristic absorption peaks at ~330nm and ~625nm (Table 4.4) The absorption peak at ~330nm can be ascribed to Π-Π^* transition of the benzenoid rings, while the peaks at the ~625nm belong to the quinoide structure of the polymer [108]. The absorbance ratio of these two peaks indicates that the doping level of PANI.

Table 4.4: The assignments of UV-visible absorption peaks of PANI samples.

Sample	λ_{330}	λ_{625}	$\Lambda_{625} / \lambda_{330}$
PANI-CI	1.97	2.23	1.13
PANIHCI-CI	1.88	1.68	0.89

It was found that in the case of these two samples of PANI the intensity ratio was smallest in the PANIHCI-CI, which meant that the doping level PANIHCI-CI was lower than PANI-CI. These results are agree with the CV measurements (Figure 4.3a) that shows higher current intensities in the case of PANI-Cl film than PANIHCI-Cl film. Also, FT-IR measurements are agreement with these results.

4.4. Electrochemical Impedance Spectroscopy of PANI-CI and PANIHCI-Cl films.

Electrochemical impedance spectroscopy (EIS) was employed to investigate the mechanistic aspects and the impedance spectra were recorded for PANI-CI and PANIHCI-CI obtained applying 8 and 16 cycles. Polymeric films are excited in the 0.0V, 0.2V and 0.7V for 2 seconds. In figure 4.7 and figure A.8, A.9, there are bode phase graphics. As seen, in the high frequency region, each film shows the capacitive property. R_s and R_{ct} values are not defined because of absence of the semi-circle in the high frequency region. The absence of semi-circle may be due to the morphology of the polymer.

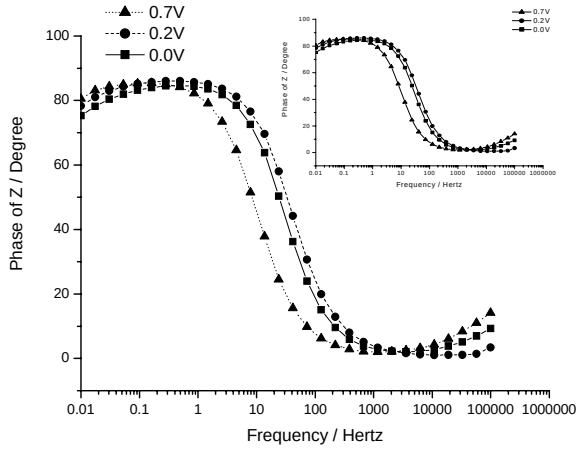

Figure 4.7: Bode phase graph of PANI-CI grown applying 8 cycles. Inset: Bode phase graph of PANIHCI-CI grown applying 8 cycles.

C_t and C_{dl} values are defined with being used other Bode phase graphs. These values are shown Table 4.5, 4.6, 4.7, and 4.8. C_t values are attributed to charge accumulation at the polymer solution interface and infer the real electroactive areas of both polymer/electrode [107]. C_{dl} values depends on the electrode potential, temperature, concentration, types of ions, oxide layers, electrode roughness, impurity adsorption[105].

Table 4.5: Impedance values for PANI-CI grown applying 8 cycles

Values	0.0 V	0.2V	0.7V
Phase/Deg.	75	78	81
C_{dl}/F	$1.9x10^{-5}$	$1.6x10^{-5}$	$5x10^{-5}$
C_t/F	$3.7x10^{-5}$	$3.2x10^{-5}$	$7.6x10^{-5}$

Table 4.6: Impedance values for PANI-CI grown applying 16 cycles

Values	0.0 V	0.2 V	0.7 V
Phase/Deg.	74	80	81
C_{dl}/F	$2.73x10^{-5}$	$2.68x10^{-5}$	$4.1x10^{-4}$
C_t/F	$5.31x10^{-5}$	$5.1x10^{-5}$	$1.27x10^{-4}$

As seen in the tables, for two PANI samples, C_{dl} and C_t values change with applied voltage and increasing thickness. These values reach the maximum at the applied 0.7 V. This reason may stems from the transformation of PANI from EB to PB which is an insulating form.

Table 4.7: Impedance values for PANIHCI-CI grown applying 8cycles.

Values	0.0 V	0.2 V	0.7 V
Phase/Deg.	77	80	77
C_{dl}/F	$1.04x10^{-5}$	$1x10^{-5}$	$5.7x10^{-5}$
C_t/F	$2.6x10^{-5}$	$2.2x10^{-5}$	$3.9x10^{-5}$

Table 4.8: Impedance values for PANIHCI-CI grown applying 16 cycles

Values	0.0 V	0.2 V	0.7 V
Phase/Deg.	73	70	79
C_{dl}/F	$6.17x10^{-6}$	$7.02x10^{-6}$	$2.81x10^{-5}$
C_t/F	$1.6x10^{-5}$	$1.86x10^{-5}$	$3.8x10^{-5}$

C_t and C_{dl} values increase with increasing film thickness in the PANI-CI sample, whereas they decrease in the PANIHCI-CI sample. This may be attributed to the ionic strength of the solution because in the second sample, there is more salt than first sample. Also, it can be reach that result, the first sample has higher electroactive surface area than the second sample.

4.5. Cyclic Voltammogram of Anilinium and Anilinium Methane Sulphanate salt

PANI-CH_3SO_3H (PANI-MS) and PANI methane sulphanate salt-CH_3SO_3H (PANIMS-MS) samples are prepared in the same way in the first experiment except that 1 M MS acid are used in this experiment. Polymer growth of these samples applying 8 cycles are shown figure 4.8 and 4.9a (see figure A.10 and A.11 for 16 cycles). As seen in the graphs, polymer growth is smoother in this polymer samples than PANI-CI (Figure 4.1 and 4.9b).

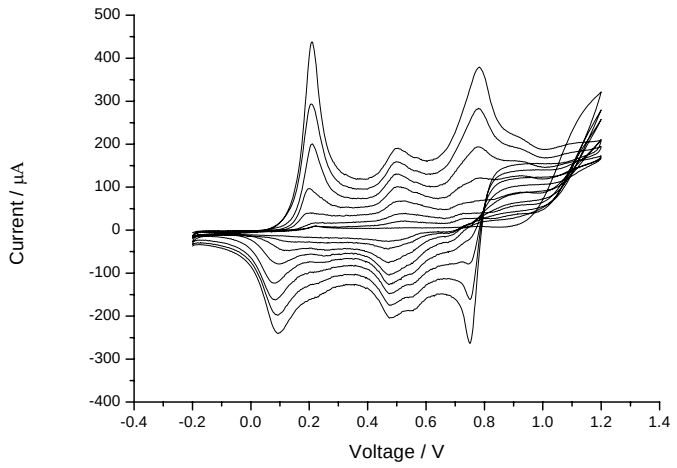

Figure 4.8: The polymer growth of ANI in 1M CH_3SO_3H at 100 mV/s scan rate applying 8 cycles.

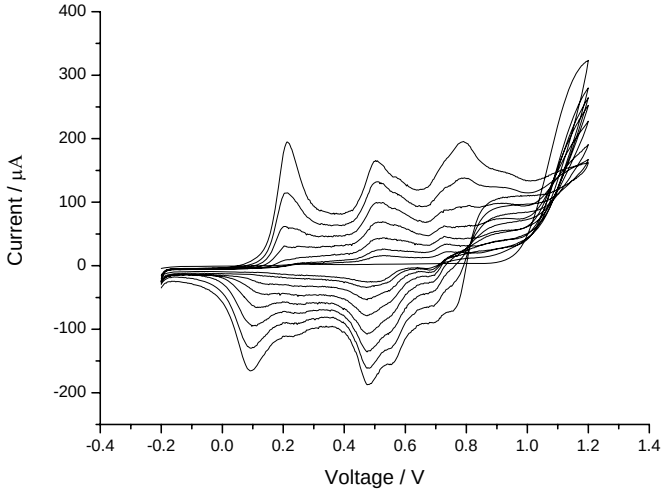

Figure 4.9a: The polymer growth of ANIMS in 1M CH_3SO_3H at 100 mV/s scan rate applying 8 cycles.

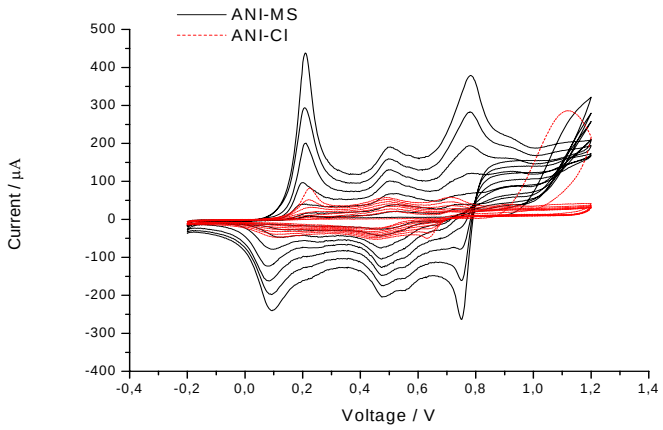

.

Figure 4.9.b: Comparison of the polymer growth of ANI-MS in 1M CH_3SO_3H and ANI-Cl in 0.5M HCl at 100 mV/s scan rate applying 8 cycles.

First and middle peaks are observed in the same potential like observed in the PANI-CI sample, only third peak is shifted to the 0.8 V (Figure 4.9 b). As it can be clearly seen higher current intensities were obtained in the case of ANI-MS than ANI-Cl. CV studies show that our films are stabile because peaks are observed even at the 1000mV/s scan rate (see figure A.12, A.13, A.14, A.15). Furthermore, the CV of PANI grown under 16 cycles has two peaks, that is, middle peak is not observed with increasing film thickness.

Figure 4.10a and 4.10b shows the comparison of CV studies of PANI-MS film and PANIMS-MS film at the 100mV/s scan rate during and after. It can be made same

explanation for these PANI samples (see section 1). PANI-MS is more conductive than PANI MS salt-MS. This comparison can be made for PANI having different thickness (see figure A.16). With the increasing film thickness, there is no change in the voltage, but current increases (Table 4.9 and 4.10).

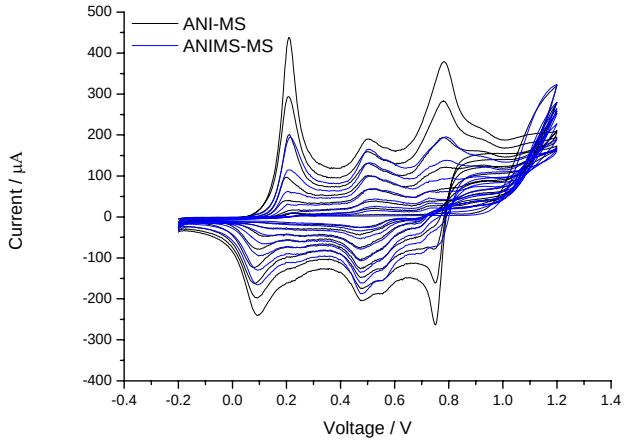

Figure 4.10a: The comparison of CV of ANI-MS and ANMS-MS applying 8 cycles at the 100mV/s scan rate.

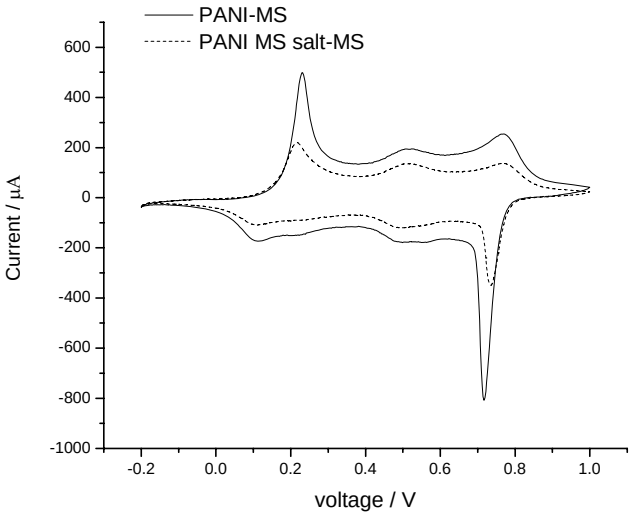

Figure 4.10b: The comparison of CV of PANI-MS and PANIMS-MS (grown applying 8 cycles) at the 100mV/s scan rate.

Table 4.9: The redox potentials and current values of PANI samples grown applying 8 cycles.

Polymer	E_{a1}/V	I_{a1}/µA	E_{a2}/V	I_{a2}/µA	E_{a3}/V	I_{a3}/µA
PANI-MS	0.22	493.24	0.5	193.7	0.77	250.45
PANIMS-MS	0.22	217.09	0.5	134.6	0.77	137.24

Table 4.10: The redox potentials and current values of PANI samples grown applying 16 cycles.

Polymer	E_{a1}/V	I_{a1}/μA	E_{a2}/V	I_{a2}/μA	E_{a3}/V	I_{a3}/μA
PANI-MS	0.27	1848.98	0.5	608.06	0.74	685.12
PANIMS-MS	0.25	1474.6	0.5	426.34	0.77	591.8

Based on the peak current I_p and the square root of scan rate from 50 to 1000mV/s^{-1}, the relationships between anodic peak currents and $\upsilon^{1/2}$ are shown in Fig. 4.10c, respectively, in which, two straight lines are obtained. This means that the electrode reaction rate of PANI films is controlled by mass transfer in the above scan potential rate range.

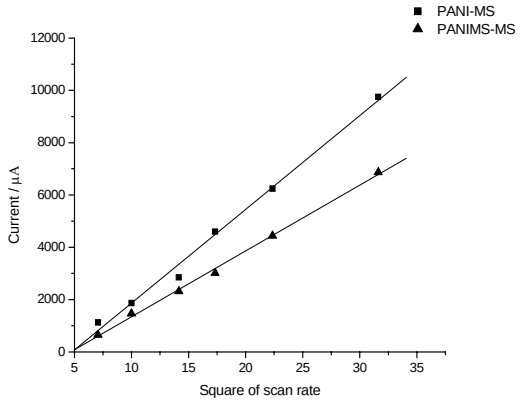

Figure 4.10c: $I_p \sim \upsilon^{1/2}$ plot for the change in the anodic peak current with the scan rate around 0.2V

4.6. Characterization of PANI-MS and PANIMS-MS with FT-IR.

Figure 4.11 shows the IR spectra of the PANI-MS and PANIMS-MS samples. When compared the IR spectrum of PANI-CI and PANICl-CI peaks were not shifted and similar behaviour observed for PANI-MS and PANIMS-MS.

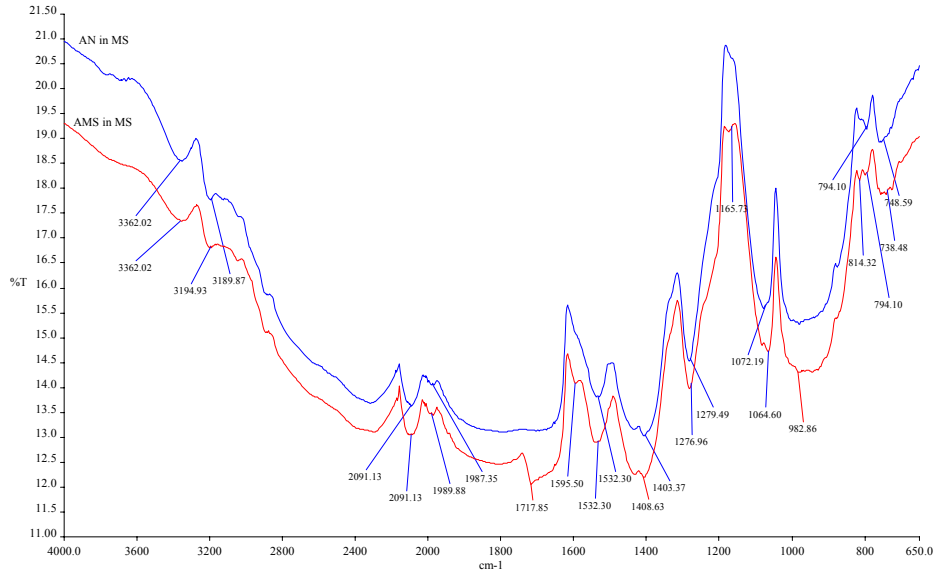

Figure 4.11: FT-IR spectra of PANI-MS and PANIMS-MS samples.

In the same way PANI-Cl and PANHCl-Cl samples, the peak intensities were obtained for PANI-MS and PANIMS-MS and collected in Table 4.11, these samples have nearly the same intensity ratio and they are in emeraldine form. Also, these samples are oxidized in the same level.

Table 4.11: The absorption intensity and R of quinoid and benzenoid units in PANI samples

Sample	$I_{1530\text{-}1550}$	$I_{1400\text{-}1450}$	R
PANI-MS	13.82	13.08	1.06
PANIMS-MS	12.92	12.27	1.05

4.7. Characterization of PANI- MS and PANIMS-MS with UV-visible absorption spectra.

Figure 4.12 shows the absorbance spectra obtained in NMP for PANI-MS and PANIMS-MS polymers. Appendix 17 and 18 shows the absorbance level in the basic and acidic medium for these polymers. From these spectra the abso.rbance ratio ($\Lambda_{625} / \lambda_{330}$) at λ_{330} and λ_{625} vere obtained and given in Table 4.12.

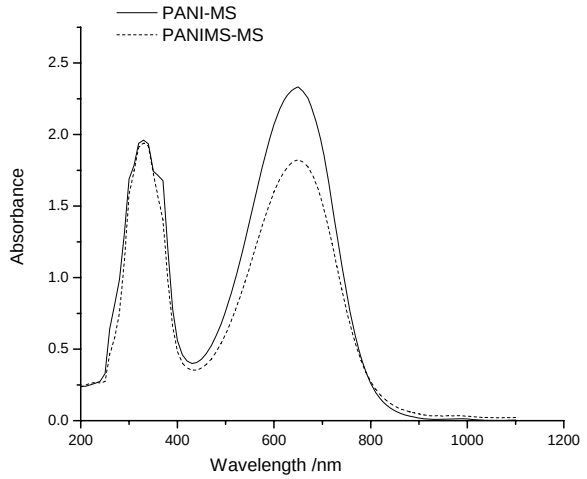

Figure 4.12: UV-visible spectra of PANI samples in the basic medium.

These values resemble the values of PANI-CI and its salt samples. PANI-MS has higher absorbance ratio than its salt form, this means it has higher doping level than its salt form.

Table 4.12: The assignment of UV absorption peaks of PANI samples.

Sample	λ_{330}	λ_{625}	$\Lambda_{625} / \lambda_{330}$
PANI-MS	1.94	2.32	1.19
PANI MS-MS	1.94	1.8	0.93

4.8 Electrochemical Impedance Spectroscopy of PANI-MS and PANIMS- MS films.

Impedance spectra were recorded for PANI-MS and PANIMS-MS for 8 and 16 cycles. These polymeric films are excited in the 0.0 V, 0.2 V and 0.8 V. In figure 4.13 and 4.14, Bode phase graphics were given. The impedance curves of electorodes at the some voltage show a distorted semi-circle in the high-frequency region due to the porosity of PANI-MS and a vertically linear spike in the low-frequency region. As seen figure A.19 and A.20, with the film thickness, linear spike in the low-frequency region are shown distinctly.

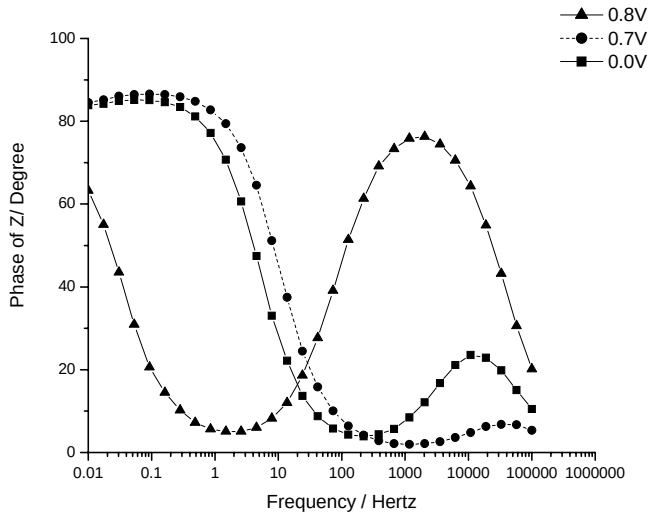

Figure 4.13: Bode phase graph of PANI-MS grown applying 8 cycles.

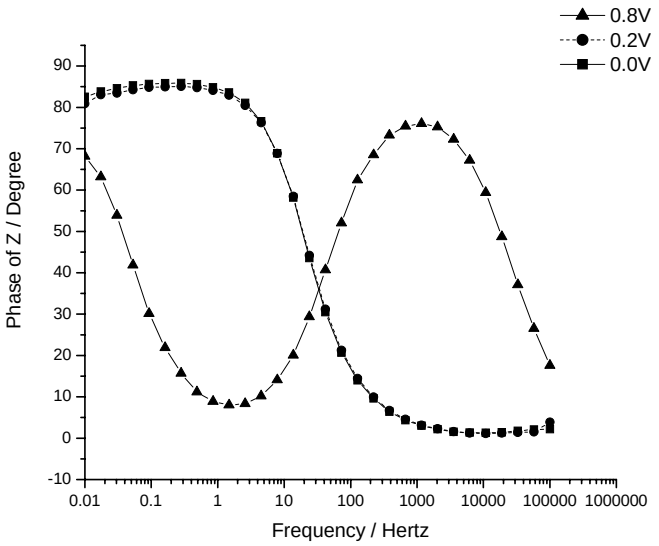

Figure 4.14: Bode phase graph of PANIMS-MS grown applying 8 cycles

Table 4.13, 4.14, 4.15, 4.16 shows the R_s, R_{ct}, C_t, Phase and C_{dl} values for each sample. R_s and R_{ct} values are defined because there are semi-circle in high frequency region for each sample. R_s is very low and approximately independent of the applied voltage and thickness, which should be a strong function of the distance between the electrodes.

Table 4.13: Impedance values for PANI-MS grown applying 8 cycles

Values	0.0 V	0.2 V	0.8 V
R_s/ohms	12.61	12	12.4
R_ct/ohms	21.82	4.12	3355
Phase/Deg.	84	85	63
C_{dl}/F	$1.52x10^{-4}$	$9.05x10^{-5}$	$2.2x10^{-4}$
C_t/F	$1.77x10^{-4}$	$1.7x10^{-4}$	$2.2x10^{-4}$
Time/sec.	$2.56x10^{-5}$	$4.84x10^{-6}$	$2.23x10^{-4}$

Table 4.14: Impedance values for PANI-MS grown applying 16 cycles

Values	0.0 V	0.2 V	0.8 V
R_s/ohms	12.1	11.8	12
R_{ct}/ohms	127	35.4	668
Phase/Deg.	84	86	66
C_{dl}/F	$4.1x10^{-3}$	$3.1x10^{-3}$	$1.2x10^{-3}$
C_t/F	$6.5x10^{-4}$	$6.81x10^{-4}$	$9.02x10^{-4}$
Time/sec.	$1.36x10^{-4}$	$4.74x10^{-5}$	$1.25x10^{-3}$

Some researches cited [106] that the ionic charge-transfer resistance, R_{ct}, decreases with the applied potentials, suggesting that the entrance of the pores becomes wider with increasing potentials, favoring the exchange of ions. However, in our experiments, at the 0.2V, R_{ct} decreases sharply. C_t and C_{dl} values increase with increasing thickness and at the 0.8 V, these values are max. at this voltage. This phenomenon is attributed to transformation of PANI, from LB to EB form, whereas, at the more positive potential 0.8 V, R_{ct} increases suddenly. Maybe, this phenomenon is attributed to transformation from EB to PB or, at the 0.8 V the pores of these samples start to become wider.

Table 4.15: Impedance values for PANIMS-MS grown applying 8 cycles

Values	**0.0 V**	**0.2 V**	**0.8 V**
Rs/ohms	-	-	0
Rct/ohms	-	-	4363
Phase/Deg.	83	81	68
Cdl/F	$3.8x10^{-5}$	3.8x10-5	$1.6x10^{-4}$
Ct/F	$9.7x10^{-5}$	$9.6x10^{-5}$	$2.19x10^{-4}$
Time/sec.	$1.6x10^{-6}$	$2.8x10^{-6}$	$2.2x10^{-3}$

Table 4.16: Impedance values for PANIMS-MS grown applying 16 cycles

Values	**0.0 V**	**0.2 V**	**0.8 V**
Rs/ohms	12.14	11.23	12.4
Rct/ohms	203.76	32.9	2501
Phase/Deg.	83	32.9	2501
Cdl/F	$2.3x10^{-3}$	$1.3x10^{-3}$	$3.2x10^{-4}$
Ct/F	$3.9x10^{-4}$	$4.3x10^{-4}$	$6.6x10^{-4}$
Time/sec.	$2.4x10^{-4}$	$4.5x10^{-5}$	$2.2x10^{-3}$

Furthermore, charge/discharge time is minimum value at the applied 0.2 V for each polymer sample. This result is expected because polymer has the highest conductivity in this voltage so that charge/discharge is very fast than the other voltages. Also, charge transfer resistance at the 0.8 V decreases with the film thickness, whereas this value at the 0.0 V and 0.2 V increases with the film thickness, this result is agreement with literature [106]

4.9. Electrical Conductivity of PANI films

Polymer films are prepared by potentiostatical way on the platinum plate electrodes at a constant voltage (0.9V) in the 0.5M HCI and 1M CH3SO3H solutions containing 0.1M aniline monomer. Obtained polymeric films are prepared as pellet. For measurement of the conductivity of a compressed pellet, a four point collinear probe method was employed. The conductivity of the compressed pellet is given by;

$$\sigma = \frac{In2}{\pi t} x \frac{I}{V} \qquad (4.1)$$

Table 4.17: Electrical conductivities of the polymers measured with four point probe solid conductivity

Sample	Conductivity (S/cm)
PANI-CI	1.1
PANIHCI-CI	0.6
PANI-MS	3.0
PANIMS-MS	1.4

Table 4.17 shows the conductivity values of the PANI films. Measurements indicated that PANI-MS film has the highest conductivity. These measurements are agreement with the CV results.

4.10. Comparison of PANI-CI and PANI-MS Films.

The conductivity of the PANI depends on the dopand. In the figure 4.15, to see the effect of dopand the CV of the PANI-HCI and PANI-MS is compared.

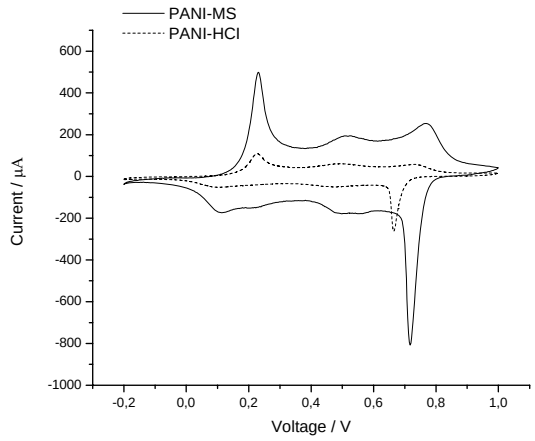

Figure 4.15: Cyclic Voltammograms of PANI-MS and PANI-HCI (grown applying 8 cycles) at 100mV/s scan rate.

Table 4.18 shows the current and voltage values for these PANI samples. Peak potentials do not change, but peak currents for PANI-MS are higher than PANI-HCI. It can be attributed that MS acid is better dopant than HCI for PANI. However, it can not be said the same thing in the case of degradation procedure. As seen in the figure 4.15, the current value in the middle peak or degradation peak is the highest in the

PANI-MS films. This indicates that PANI degradation is minimum in HCI doped with PANI and this leads to a better quality of PANI films.

Table 4.18: The redox potentials and current values of PANI grown applying 8 cycles.

Polymer	Media	E_{a1}/V	I_{a1}/µA	E_{a2}/V	I_{a2}/µA	E_{a3}/V	I_{a3}/µA
PANI	HCI	0.22	108.07	0.49	60.91	0.73	56.6
PANI	MS	0.22	493.24	0.5	193.7	0.77	250.45

EIS measurements show that the MS is a good dopant for PANI too. Phase degree is very close to the 90 degree for MS and C_t value is high for MS. That means, PANI doped MS has very high surface area and higher capacitive property.

It can be reached these results with different experiment which CV of the PANI sample is analyzed with two different electrolytes. Figure 4.16 shows the CV of the PANI-MS sample analyzed in the HCI and MS acid.

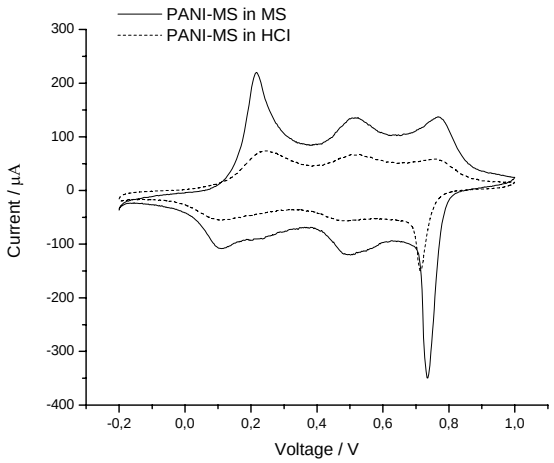

Figure 4.16: Cyclic Voltommogram of the PANI-MS in 0.5M HCI and 1M MS monomer free solutions.

4.11. Morphological Analysis of the PANI-CI and PANI-MS films.

The morphology of PANI samples were investigated by scanning electron microscopy (SEM). Figure 4.17 and 4.18 shows the PANI-HCI and PANI-MS films obtained potentiostaticly at 0.9V. It is clear from the SEM image of PANI-HCI that the sample is smooth and homogeneous as said in the earlier studies [109]. However, PANI-MS film surface has the same globular and porous structure. In the impedance measurements, it could be said that in the high frequency region there was no semi-

circle for PANI-HCI films. SEM images verify this result. In the same way, semi-circle in the high frequency region for PANI-MS film depends on the porous surface of the film, as seen in the SEM image.

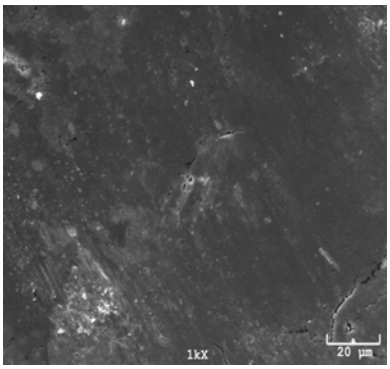

(a)

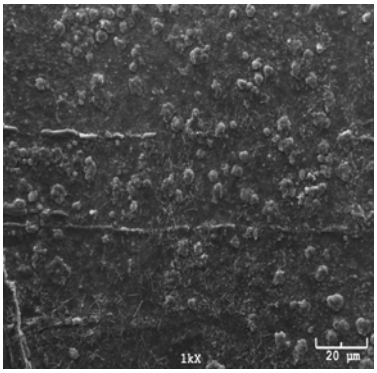

(b)

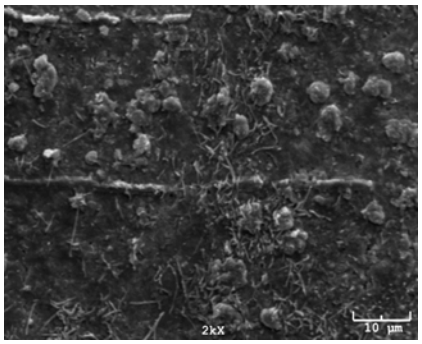

(c)

Figure 4.17: (a) SEM images of PANI-CI film (b) SEM images of PANI-MS film with growing 1kx scale (c) SEM images of PANI-MS film with growing 2kx scale

4.12 An In-situ UV-Vis Spectroelectrochemical Investigation of PANI-MS Film

The color of PANI film in the electrolyte solution can be quickly changed with the applied potential. Thus, this property is very favorable to its application in electrochromic devices [110]. In situ technique was used to examine electrochromic properties of PANI in our experiment.

The electrolysis cell for the electrochemical polymerization of aniline consisted of indium-tin oxide (ITO) as working electrode, Pt as a counter electrode and Ag as a reference electrode. PANI-MS film is deposited on (ITO) glass sheet electrodes at a constant potential of 1.1V.

The in situ spectroelectrochemical experiments of PANI-MS film were carried out by UV-vis spectroelectrochemistry. The reference cell contained an MS acid solution. The measurements of the visible spectra were performed at different potentials with an interval of around 2 min between two measurements.

Figure 4.18 shows UV-vis spectra of PANI-MS film on ITO glass electrode at different electrode potential values.

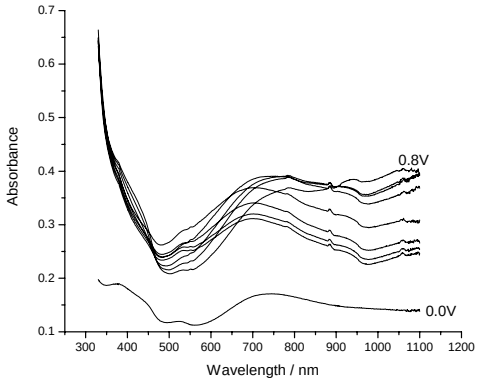

Figure 4.18: UV-vis spectra of a PANI-MS coated ITO glass electrode, obtained at different electrode potential values, ranging from 0.0 to 0.8V at every 0.1V.

There is a one shoulder at around 750 nm and there is an increase in absorbance with the increasing applied voltage. This is ascribed to formation of the charge carriers in the polymer chains.

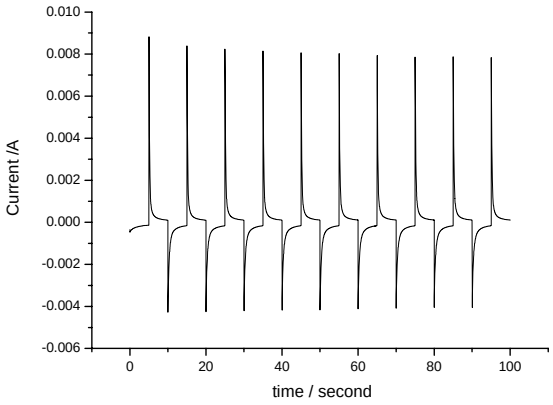

Figure 4.19: Current vs. time profiles, obtained with a PANI-MS coated electrode by stepping the electrode potential to -0.6V and 0.8V.

Also, figure 4.19 shows the switch time between 0.8V and -0.6V. As seen, switch time is nearly 1 second.

5. CONCLUSIONS

In conclusion, thin films obtained from aniline monomer are preferred to the aniline salt because of the higher current intensities that corresponds to doping degree of the PANI-Cl than PANIHCI-Cl. Also, PANI-Cl has higher capacitance values than PANIHCI-Cl so PANI-Cl is good choice for the supercapacitor applications. Increase in thickness is good effect on the PANI samples like as high conductivity. However, capacitance values for these polymer samples decrease with increasing thickness. Polymer films show linear dependence to scan rates and they are stabile until the high scan rate which indicates a high electron transfer mechanism.

It can be reached the same conclusion for the thin films obtained doped with methane sulphonice acid. PANI obtained from aniline in methane sulphonice acide is higher conductivity and capacitance values than PANIMS-MS films obtained from ANI-MS salts in MS. There is one difference from the PANI samples doped with HCI, this difference is that in the PANI samples doped with MS, capacitance values increase with increasing film thickness. Also, sharp increase in charge transfer resistance value at the applied 0.7 V is suitable for PANI`s insulating form in this voltage. For each sample, charge/discharge time increase with increasing film thickness. This time is the lowest value in the PANI-MS obtained from 8 cycles, so films obtained 8 cycles is more preferred from than the film obtained 16 cycles. Because the lowest charge/discharge time this is, the best film.

Also, the samples doped with MS are higher conductivity than the samples doped with HCI. It can be concluded that MS is better dopant from the HCI. Furthermore, MS is an organic acid and HCI is a inorganic acid, so it can be said that organic acids are more appropriate media than the inorganic acids. Besides, films obtained MS is smoother than films obtained HCI with respect to the polymer growth figures of polymers. These results are valid for their salt forms.

SEM images of the samples show that PANI-CI films have smoother surface than PANI-MS films. Surface of the PANI-MS films are porous and globular, whereas

surface of the PANI-MS films are homogenous and smooth. SEM images results are agreement with the empedance results, because charge resistance values depend on the surface morphology.

To solid state conductiviy measurements, polyaniline obtained in MS acids has very high values, 3 S/cm^{-1} and this result are agreement with the CV results.

Finally, in-situ spectroelectrochemical measurement showed the formation of the charge carriers in the polymer chains and also, the transformation of color change in the PANI-MS film happens in nearly 1 second and this time is not good for electrochromic application.

REFERENCES

[1] Bao, Z., Balapur, D.A., Loverigen, J.A., 1996. Soluble and processable regioregular poly(3-hexylthiophene) for thin film field-effect transistor applications with high mobility, *Appl. Phys. Lett.* **69**, 4108-4112.

[2] Yu, G., Pakabaz P., Heeger, J.A., 1994. Semiconducting polymer diodes: Large size, low cost photodetectors with excellent visible-ultraviolet sensitivity, *Appl. Phys. Lett.* **64**, 3422-3432.

[3] Bregglem, M., Ingnas, O., Gustabsson, G., Rassuenssen, J., Anderson, R.M., Hiertberg, T., Wernerstern, O., 1994. Light-emitting diodes with variable colors from polymer blends**,** *Nature (London)*, **372**, 444-452.

[4] Burroughes, H., Bradeley, C.D.D., Brown, R.A., Marks, N.R., Mackas, K., Friends, H.R., Burns, L.P., Holmers, B.A., 1990. Light-emitting diodes based on conjugated polymers, *Nature (London),* **347**, 539.

[5] Brable, J.C., Saricifici, S.N., Hummelen, C.J., 2001. Plastic Solar Cells, Adv., *Functional Materials*, **11**, 15-26.

[6] Prasad, R.K., Munichandraiah, N., 2001. Potentiodynamic deposition of polyaniline on non-platinum metals and characterization, *Synth.. Met*., 1**23**, 459-468.

[7] Martyak, M.N., McAndrew, P., McCaskie, E.J., Dijon, J., 2002. Electrochemical polymerization of aniline from an oxalic acid medium**,** *Prog.Org. Coat.*, **45**, 23-35.

[8] Lacroix, C.J., Diaz, F.A., 1988. Electrolyte Effects on the Switching Reaction of Polyaniline, *J. Eletrochem. Soc*., **135**, 1457-1466.

[9] Kanatzidis, G.M., 1990. *Chem. & Eng. News,* **68**, 37.

[10] Yoshino, K., Tada, K., Hirohata, M., Kajii, H., Hironaka, Y., Tada, N., Kaneuchi, Y., Yoshida, M., Fujii, A., Hamaguchi, M., Araki, H., 1997. Novel properties of molecularly doped conducting polymers and junction devices, *Synth. Met.,* **84**, 477-490.

[11] Misra, K.C.S., Ram, K.M., Pandey, S.S., Malhotra, D.B., Chandra, S.,1992. vacuum-deposited metal/polyaniline Schottky device, *Appl. Phys. Lett.* **61**, 1219-1230.

[12] Alva, S.K., Kumar, J., Marx, A.K., Tripathy, K.S., 1997. Enzymatic Synthesis and Characterization of a Novel Water-Soluble Polyaniline Poly(2,5diaminobenzenesulfonate), *Macromolecules*, **30**, 4024-4035.

[13] LaCroix, C.J., Hoshino, Y., 1993. Coulombic irreversibility at polyaniline-coated electrodes by electrochemical switching, *Electrochim. Act.,* **38**, 1711-1723.

[14] Huang, S.W., Humphery, D.B., and MacDiarmid, G.A., 1986. Polyaniline, a novel conducting polymer. Morphology and chemistry of its oxidation and reduction in aqueous electrolytes**,** *J. Chem. Soc. Faraday Trans. I*, **82,** 2385-2393.

[15] Andreasen, G., Arvia, J.A., Salvarezza, C.R , Vela, E.M, 1996. Dynamic scaling analysis of scanning force microscopy images of electrochemically formed polyaniline films in the oxidized form scale-dependent roughening kinetics, *J. Chem. Soc., FaradayTrans.,* **2**, 4093- 5000.

[16] Rourke, F., Crayston, A.J., 1993. Cyclic voltammetry and morphology of polyaniline-coated electrodes containing $[Fe(CN)_6]^{3-/4-}$ ions, *J. Chem. Soc. Faraday Trans.,* **89**, 295-303.

[17] Kalaji, M., Peter, M.L., 1991. Optical and electrical response of polyaniline films, *J.Chem.Soc.Faraday trans*., **87**, 853-870.

[18] Inzelt, G., Lang, G., Kertsz, V., and Bacskai, J., 1993. Effect of the temperature on the conductivity and capacitance of poly(aniline) film electrodes, *Electrichim. Act.,* **38,** 2503-2512.

[19] Matveeva, S.E., Calleja, D.R., and Parkhutik, P.V., 1996. **I**mpedance study of chemically synthesized emeraldine form of polyaniline, *Electrochim. Act.,* **41**, 1351-1365.

[20] Benyaich, A., Deslouis, C., Moustafid, E.T., Musiani, M.M., and Tribollet, B., 1996. Electrochemical properties of PANI films for different counter-ions in acidic pH analysed by impedance techniques, *Electrochim. Act.,* **41**, 1781-1794.

[21] Komura, T., Sakabayashi, H., and Takahashi, K., 1995. Electrochemical Impedance Study and Characteristics of Polyaniline Film Electrodes, *Bull. Chem. Soc. Jpn.,* **68**, 476-480.

[22] Grzeszezuk M. and Olszak, Z.G., 1993. Ionic transport in polyaniline film electrodes: an impedance study**,** *J. Electroanal. Chem.,* **359,** 161-175.

[23] Camalet, L.J., Lacroix, C.J., Aeiyach, S., Ching, C.K., Lacaze, C.P.,1998. Electrosynthesis of adherent polyaniline films on iron and mild steel in aqueous oxalic acid medium, *Synth. Met.* **93,** 133-151.

[24] Sazou, D., Georgolios, C., 1997. Formation of conducting polyaniline coatings on iron surfaces by electropolymerization of aniline in aqueous solutions, *J. Electroanal. Chem.,* **429**, 81.

[25] Skotheim, T. A., 1986. Handbook of Conducting Polymers, Marcel Dekker, Vols. 1-2, New York.

[26] MacDiarmid, G.A., Chiang, C.J., Richter, F.A., and Epstein, J.A., 1987. Polyaniline: a new concept in conducting polymers, *Synth. Met*., **18,** 285-300 .

[27] Epstein, J.A., Ginder, M.J., Zuo, F., Woo, S.H., Tanner, B.D., Richter, F.A., Angelopoulos, M., Huang, S.W., and MacDiarmid, G.A., 1987. Insulator-to-metal transition in polyaniline: Effect of protonation in emeraldine, *Synth. Met.,* **21,** 63-75**.**

[28] MacDiarmid, G.A., and Epstein, J.A., 1989. **Polyanilines: a novel class of conducting polymers** Faraday Discuss., *Chem. Soc*., **88**, 317-325.

[29] Frommer, J.E., Chance, R.R., 1990. Encyclopedia of Polym. Sci. Eng., 5,462-507.

[30] Chance, R., Boudreaux, H., Eckhardt, R., Elsenbaumer, J., Frommer, J., Redas, J., Silbey, R., Ladik, J., Andre, J.,1984. Quantum Chemistry of Polymers-Solid State Aspects, D. Reidel Publishing Co., 221-233.

[31] Trivedi, D., 1997. In Handbook of Organic Conductive Molecules and Polymers, H.S.Nalwa (Ed.), Vol. 2, pp. 506-572, John Wiley & Sons Ltd., Chichester.

[32] Oyama, N., Tatsuma, T., Sato, T., Sotomura, T., 1995. *Nature*, **373,** 598.

[33] Stilwell, E.D., Park, M.S., 1988. **Electrochemistry of Conductive Polymers**, *J. Electrochem. Soc*.,**135**, 2254-2271.

[34] Christie, S., Scorsone, E., Persaud, K., Kvasnik, F., 2003. Remote detection of gaseous ammonia using the near infrared transmission properties of polyaniline *Sens. Actuators B*, **90,**163-182.

[35] Jianming, Y., El-Sherif, A.M., 2003. Fiber-optic chemical sensor using polyaniline as modified cladding material**,** *Sensor J*., **3**, 5-13.

[36] Prasad, R.K., Munichandraiah, N., 2002. *Electrochem. Solid-State Lett*., **5**, 271-292.

[37] Sharma, P.R., Raghuvanshi, S.M., Bhavsar, V.S., Patil, R.A., Misra, K.C.S., 2002. Polyaniline thin film optical waveguides for integrated optics and VLSI prepared by vacuum evaporation technique, *Polym. Adv. Technol.* 13, 475-480.

[38] Fahlman, M., Jasty, S., Epstein, J.A., 1997. Corrosion protection of iron/steel by emeraldine base polyaniline: an X-ray photoelectron spectroscopy study, *Synth. Met.* 85,1323-1331.

[39] Kinlen, J.P., Menon, V., Ding, Y., 1999. A Mechanistic Investigation of Polyaniline Corrosion Protection Using the Scanning Reference Electrode Technique, *J. Electrochem. Soc., 146***,** 3690-3701.

[40] Cortevieille, D., Mahaute, L. A., Chailloui, C., Mirebeau, P., Demay, N.J., 1999. Industrial applications of polyaniline**,** *Synth. Met.,* **101,** 703-710.

[41] Duek, A.E., Paoli, A.M., Mastragostino, M., 1993. *Adv. Mater.,* **5,** 349-357.

[42] Bhattacharya, A., De, A., 1996. Conducting composites of polypyrrole and polyaniline a review**,** *Prog. Solid St. Chem.,* **24,** 141-153.

[43] Canobre, C.S., Biaggio, R.S., Rocha-Filho, C.R., Bocchi, N., 2003. Influence of the preparation procedure on the electrochemical properties of Pani(DMcT-Cu ion)/carbon fiber composites, *J.Braz. Chem. Soc.*, **14,** 621-635.

[44] Dalmolin, C., Canobre, C. S., Biaggio, S. R., Rocha- Filho, R. C., Bocchi, N., 2004, Electropolymerization of polyaniline on high surface area carbon substrates, J. Electroanal. Chem.

[45] Efremova, A., Regis, A., Arsov, Lj., 1994. Electrochemical formation and deposition of polyaniline on electrode surface; *In situ* raman spectroscopical study, *Electrochim. Acta,* **39,** 839-853**.**

[46] Arsov, Lj., 1998. Electrochemical study of polyaniline deposited on a titanium surface, *J. Solid State Electrochem., 2,* 266-281.

[47] Efremova, A., Arsov, Lj., 1992. *J. Serb. Chem. Soc.*, **57**, 127-138.

[48] Mandic, Z., Duic, L., and Kovacicek, F., 1996, The Influence of Counter-ions on nucleation and growth of electrochemically synthesized polyaniline films, *Electrochim. Acta,* **42,** 1389-1402.

[49] Zhu, C., Wang, C., Yang, L., Bai, C., Wang, F., 1999. Dopant dimension influence on polyaniline film structure, *Appl. Phys. A,* **68**, 435-453.

[50] Trivedi, D.,1988. Influence of the anion on polyaniline**,** *J. Solid State Electrochem*., **2,** 85-91.

[51] Zhang, Q.A., Cui, Q.C., Lee, Y.J., 1995. Electrochemical degradation of polyaniline in $HClO_4$ and H_2SO_4 , *Synth. Met.,* **72,** 217-225**.**

[52] Andrade, T.G., Aguirre, J.M., Biaggio, R.S., 1988, Influence of the First Potential Scan on the Morphology and Electrical Properties of Potentiodynamically Grown Polyaniline Films, *Electrochim. Acta,* **44,** 633-642.

[53] Mu, S., 2005. Polyaniline with Two Types of Functional Groups:Preparation and Characteristics, *Macromolecular Chemistry and Physics,* **206,** 689-695.

[54] Chen, C.W., Wen, C.T., Gopalan, A., 2002. Negative Capacitance for Polyaniline: an Analysis via Electrochemical Impeance Spectroscopy, *Synth. Met.,* **128,** 179-189.

[55] Fiordiponti, P., Pistoia, G., 1989. An impedance study of polyaniline films in aqueous and organic solutions, **Electrochim. Acta, 34,** 215-224**.**

[56] Genz, O., Lohrengel, M.M, Schultze, W.J., 1994. Potentiostatic pulse and impedance investigations of the redox process in polyaniline films, *Electrochim. Acta,* **39,** 171-185.

[57] Deslouis, C., Musiani, M.M., Tribollet, B., Vorotyntsev, A.M., 1995. J. *Electrochem. Soc.,* **142,** 1902-1911**.**

[58] Grzeszczuk, M., Poks, P., 1995. Analysis of charge transport impedance in the reduction of thin films of conducting polyaniline in aqueous trichloroacetic acid solutions, *J. Electroanal. Chem.,* **387,** 79-87.

[59] Roßberg, K., Paasch, G., Dunsch, L., Ludwig, S., 1998. The influence of porosity and the nature of the charge storage capacitance on the impedance behaviour of electropolymerized polyaniline films, *J. Electroanal. Chem.,* **443,** 49-58.

[60] Lubert, H.K., Dunsch, L., 1998. The influence of protons on the impedance of polyaniline films, *Electrochim. Acta,* **43,** 813-823.

[61] Schrebler, R., G´omez, H., C´ordova, R., Gassa, M.L., Vilche, R.J., 1998. Study of the aniline oxidation process and characterization of Pani films by electrochemical impedance spectroscopy, *Synth. Met.,* **93,** 187-195.

[62 Dinh, N.H., Van´ysek, P., Birss, I.V., 1999. The Effect of Film Thickness and Growth Method on Polyaniline Film Properties, *J. Electrochem. Soc.,* **146,** 3324-3337**.**

[63] Gabrielli, C., Keddam, M., Nadi, N., Perrot, H., 2000. Ions and solvent transport across conducting polymers investigated by ac electrogravimetry. Application to polyaniline, *J. Electroanal.Chem.,* **485,** 101-115.

[64] Matveeva, S.E., Gonzales-Tejera, J.M., 2000. Impedance Study of theCharge-Transfer Interaction Between the Polyaniline Chain and Redox Pair in Solution, *J. Electrochem. Soc.,* **147,** 1213-1224.

[65] Dinh, N.H., Birss, I.V., 2000. Effect of Substrate on Polyaniline Film Properties A Cyclic Voltammetry and Impedance Study, *J. Electrochem. Soc.,***147**, 3775-3787.

[66] Hu, C.C., Chu, H.C., 2001. Electrochemical impedance characterization of polyaniline-coated graphite electrodes for electrochemical capacitors effects of film coverage/thickness and anions, *J. Electroanal. Chem.,* **503,** 105-113.

[67] Mondal, K.S., Prasad, R.K., Munichandraiah, N., 2005. Analysis of electrochemical impedance of polyaniline films prepared by galvanostatic, potentiostatic and potentiodynamic methods, *Synth. Met.,* **148,** 275-286.

[68] Rodriguez P.J.M., Bandey, L.H., Tucceri, I.R., Florit, I.M., Posadas, D.,Hillman, R.A., 1998. Charge transfer in poly(*o*-toluidine) gold modified electrodes. An EIS study of the reduced state, *J.Electroanal. Chem.,* **455**, 49-55.

[69] Gazotti Jr. A.W., Matencio, T., Paoli, D.A.M., 1998. Electrochemical impedance spectroscopy studies for chemically prepared poly(*o*-methoxyaniline) doped with functionalized acids, *Electrochim. Acta,* **43,** 457-465.

[70] Florit, I.M., Posadas, D., Mollina, V.F., Andrade, M.E., 1999. The Effect of Temperature on the Impedance of Poly-*o*-toluidine in 3.7 M H_2SO_4, *J. Electrochem.Soc*., **146,** 2592-3001.

[71] Hillman, 1999. Film thickness and electrolyte concentration effects on the EIS response of Poly-(*o*-toluidine) in the conducting state, *Electrochim. Acta,* **44,** 2073-2084.

[72] Lindfors, T., Ivaska, A., 2002. pH Sensitivity of polyaniline and its substituted derivatives, *J. Electroanal. Chem*., 531, 43-52.

[73] Stejskal, J., Kratochvil, P., Jenkins, D.A.,1996. The formation of polyaniline and the nature of its structures, *Polymer*, **37,** 367-375**.**

[74] Trivedi, D., 1997. In Handbook of Organic Conductive Molecules and Polymers, H. S. Nalwa (Ed.), Vol. 2, pp. 505–572, Wiley, Chichester.

[75] Gospodinova, N., Terlemezyan, L., 1998. Conducting polymers prepared by oxidative polymerization: polyaniline, *Polym. Sci.,* **23,** 1443-1484.

[76] Quillard, S., Berrada, K., Louarn, G., Lefrant, S., Lapkowski, P., Pro´n, A., 1995. *New J. Chem*., **19,** 365-372.

[77] Campos, M., Bello, B., 1997. Mechanism of Conduction in Doped Polyaniline, *Journal Physics*, **30,** 1531-1535.

[78] McManus, M.P., Cushman, J.R., and Yang, C.S., 1987. Influence of oxidation and protonation on the electrical conductivity of polyaniline, *Journal of Physical Chem.,* **91,** 744-753.

[79] Yu L.T., Borredon M.S., Jozefowicz M., Belorgey G. and Buvet R., 1987. *J. Polym. Sci.,* **10,** 293-300.

[80] Nunziante, P. and Pistoia, G., 1989. Factors affecting the growth of thick polyaniline films by the cyclic voltammetry technique, *Electrochim. Act.,* **34**, 223-235**.**

[81] Kazarinov, E.V., Andreev, N.V., Spytsin, A.M., and Shlepakov, V.A., 1990. *Electrochim. Act.,* **35,** 899-309.

[82] Inzelt, G., Horanyi, G., 1990. Some problems connected with the study and evaluation of the effect of pH and electrolyte concentration on the behaviour of polyaniline film electrodes, *Electrochim. Act.,* **35,** 27-46.

[83] Wei, Y., Sun, Y., Jang, W.G., and Tung, X.,1990. Effects of *p*-aminodiphenylamine on electrochemical polymerization of aniline, *J. Polym. Sci.,Polym. Lett.*, **28**, 81-90.

[84] Karakisla, M., Sacak, M., Erdem, E., Akbulut, U., 1997. Synthesis and Characterization of Malonic Acid-Doped Polyaniline, *J .App. Electrochem.***, 27,** 309-316.

[85] Cui, Y.S., Park, M.S., 1999. Electrochemistry of conductive polymers XXIII: polyaniline growth studied by electrochemical quartz crystal microbalance measurements, *Synth. Met.*, **105**, 91-100**.**

[86] Doic, L., Mandic, Z., Kovac, 1995. Polymer-dimer distribution in the electrochemical synthesis of polyaniline**,** *Electrochim. Acta,* **40,** 1681.

[87] Abdiryim, T., Gang, X.Z., Jamal, R., 2005. Comparative Studies of Solid-State Sythesized Polyaniline Doped with Inorganic Acids, *Materials Chemistry and Physics,* **90,** 367-372.

[88] Arsov, Lj., Plieth, W., Kobmehl, G.,1998. Electrochemical and Raman spectroscopic study of polyaniline; influence of the potential on the degradation of polyaniline, *J. Solid State Electrochem.,* **2,** 355-361.

[89] Buzarovska, A., Arsova, I., and Arsov, L., 2001. Electrochemical Synthesis of Poly(2MethylAniline), Electrochemical and Spectroscopic Characterization, J. Serb. Soc., 66, 27-37.

[90] Schmidt, E., 1986. Inhomogeneous electrodes and polarization model of the partially blocked reversible metal ion electrode, *Electrochim. Acta,* **31,** 1041-1052.

[91] Cai, M.; Park, S.-M., 1996**.** Spectroelectrochemical Studies on Dissolution and Passivation of Zinc Electrodes in Alkaline Solutions, *J. Electrochem. Soc*.**, 143,** 2125-2134.

[92] Cha, D. K.; Park, S.-M., 1997. Electrochemical Oxidation of $Mn(OH)_2$ in Alkaline Media, *J. Electrochem. Soc.,* **144,** 2573-2584.

[93] Lay, P., 1985. An a.c. impedance study of steel in concrete, *J. Appl. Electrochem.,* **15**, 755-766**.**

[94] Cha, D. K.; Park, S.-M., 1998. Electrochemical characterization of polyethylene glycols as solid polymer electrolytes, *J. Electroanal.Chem.*, **459,** 135-147.

[95] Piao, T., 1999. Intercalation of Lithium Ions into Graphite Electrodes Studied by AC Impedance Measurements, *J. Electrochem. Soc.,* **146**, 2794-3001.

[96] Kim, Y.-O.; Park, S.-M., 2001. Intercalation Mechanism of Lithium Ions into Graphite Layers Studied by Nuclear Magnetic Resonance andImpedance Experiments, *J. Electrochem. Soc*., **148**, A194**.**

[97] Gabrielli, C., Haas, O., Takenouti, H. J., 1987. Impedance analysis of electrodes modified with a reversible redox polymer film, *Appl. Electrochem.,* **17,** 82-90.

[98] Johnson, B. J., Park, S.-M. 1996. Electrochemistry of Conductive Polymer, J. *Electrochem. Soc.,* **143,** 1269-178.

[99] Lee, J.-Y., Park, S.M., 2000. Electrochemistry of Conductive Polymers. XXIV. Polypyrrole Films Grown at Electrodes Modified with β-Cyclodextrin Molecular Templates, *J. Electrochem. Soc.,* **147,** 4189**.**

[100] Gabrielli, C., 1990. Use and applications of electrochemical impedance spectroscopy, Technical Report, Schlumberger Technologies, Farnborough, p. II.38.

[101] Darowicki, K., Kawula, J., 2004. Impedance Characterization of the Process of Polyaniline First Redox transformation, *Electrocimica Acta,* **49,** 4829-4839.

[102] Electrochemical Impedance Spectrum Primier of the Gamry Instruments.

[103] Girija, C.T., Sangaranarayanan, V.M., 2006, Polyaniline-Based Nickel Electrodes for Electrochemical Supercapacitors-Influence of Triton X-100*, Journal of Power Sources*.

[104] Barsoukov, E., Macdonald, R.J., 2005. Impedance Spectroscopy, pp. 478, Wiley-Interscience, New Jersey.

[105] Help menu of PowerSuite software in PARSTAT 2263 Potentiostat.

[106] Girija, C.T., Sangaranarayanan, V.M., 2006. Investigation of Polyaniline-Coated Stainless Steel Electrodes for Electrochemical Supercapacitors, *Synth. Met.*.

[107] Burke, A., 2000. Ultracapacitors: why, how, and where is the technology, J. *Power Sources*, **91,** 37-46.

[108] Yasuda, T., Yamaguchi, I., Yamamato, T., 2003. *Synth. Met.*, **10405,** 1-4.

[109] Raghavendra, C.S., Khasim, S., Revanasiddappa, M., Prasad, A., Kulkarni, B.A., 2003. Synthesis, characterization, and low frequency a.c. condution of polyaniline/fly ash composites, *Bull. Met. Sci.*, **26,** 733-739

[110] Li, C., Mu, S., 2004. Electrochromic properties of sulfonic acid ring-substituted polyaniline in aquous and non-aquous media, *Synth. Met.*,**144,** 143-149.

APPENDICES

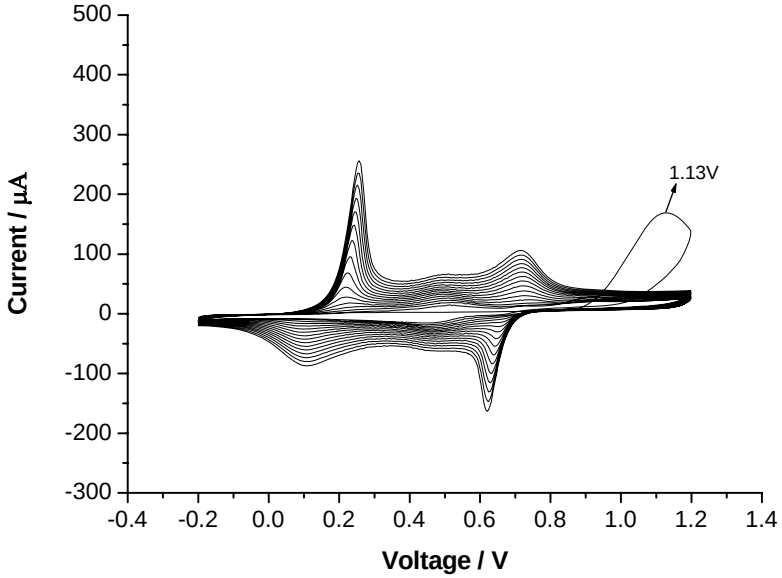

Figure A.1: The polymer growth of ANI in 0.5M HCI at 100 mV/s scan rate applying 16 cycles.

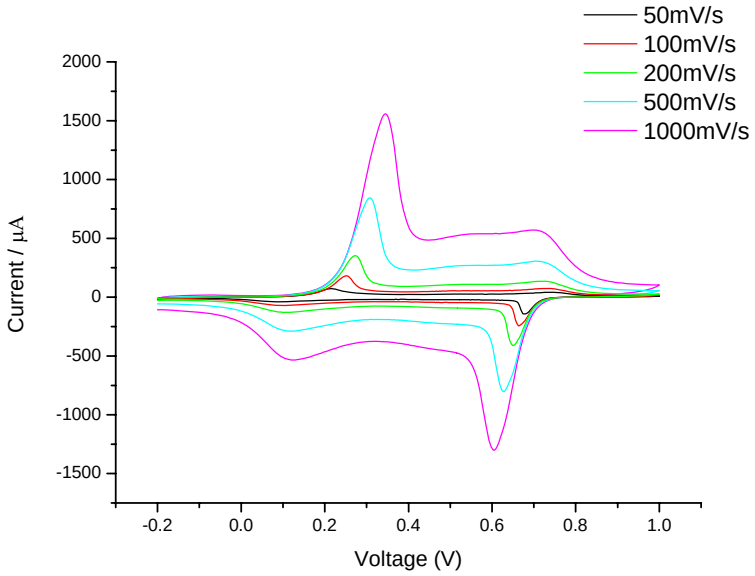

Figure A.2: Scan rate dependence of PANI-CI film (grown applying 16 cycles) in monomer free electrolyte at the different scan rates.

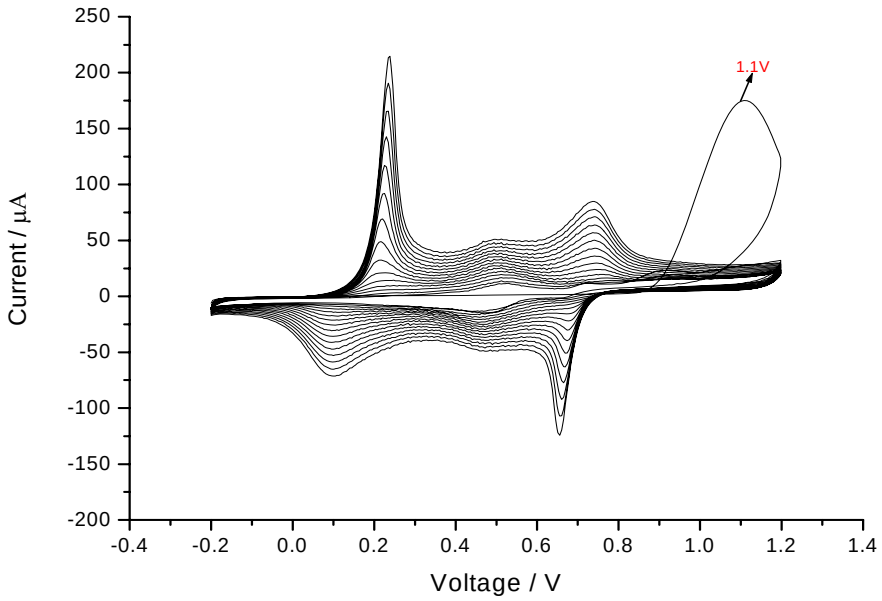

Figure A.3: The polymer growth of ANICI in 0.5M HCI at 100 mV/s scan rate applying 16 cycles.

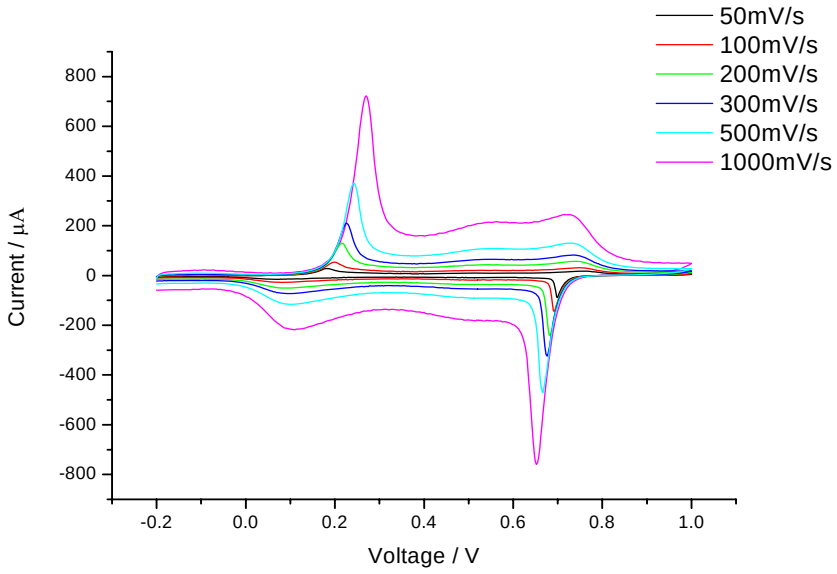

Figure A.4: Scan rate dependence of PANIHCI-CI (grown applying 16 cycles) in monomer free electrolyte at the different scan rates.

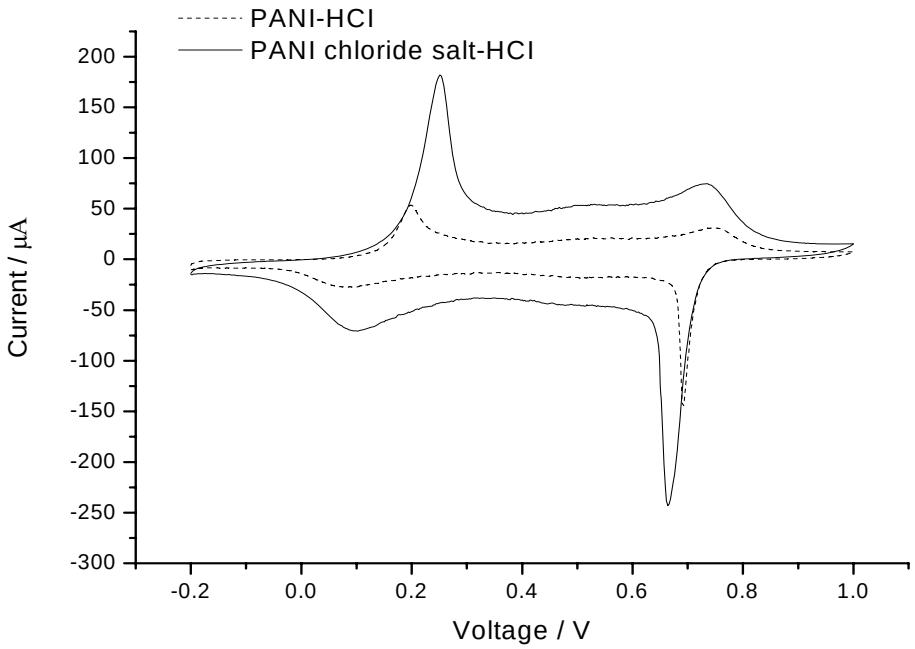

Figure A.5: The comparison of CV of PANI-CI and PANIHCI-CI grown applying 16 cycles at the 100mV/s scan rate

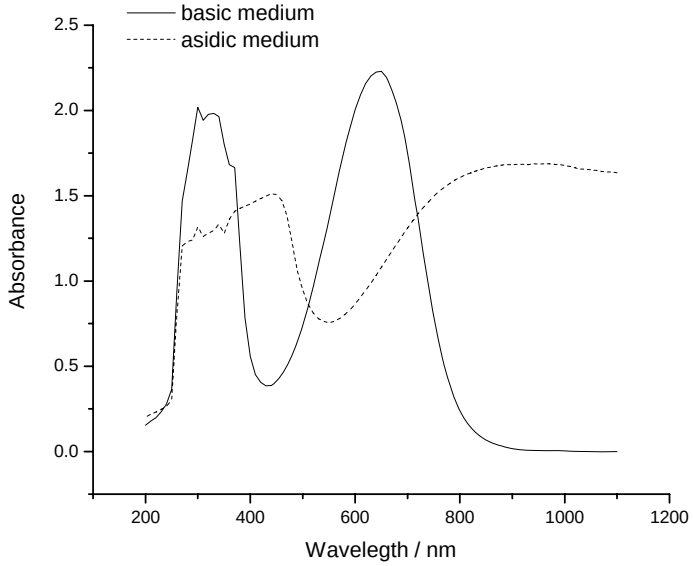

Figure A.6: UV-visible spectra of PANI-CI sample in the basic and acidic medium.

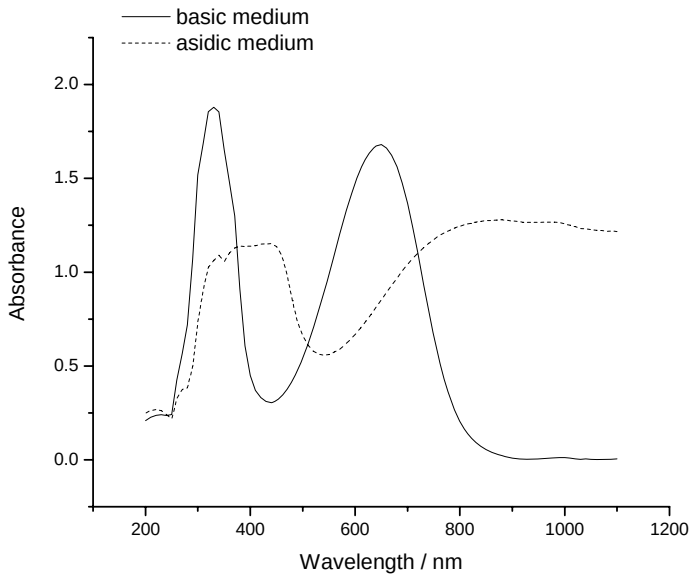

Figure A.7: UV-visible spectra of PANIHCI-CI sample in the basic and acidic medium.

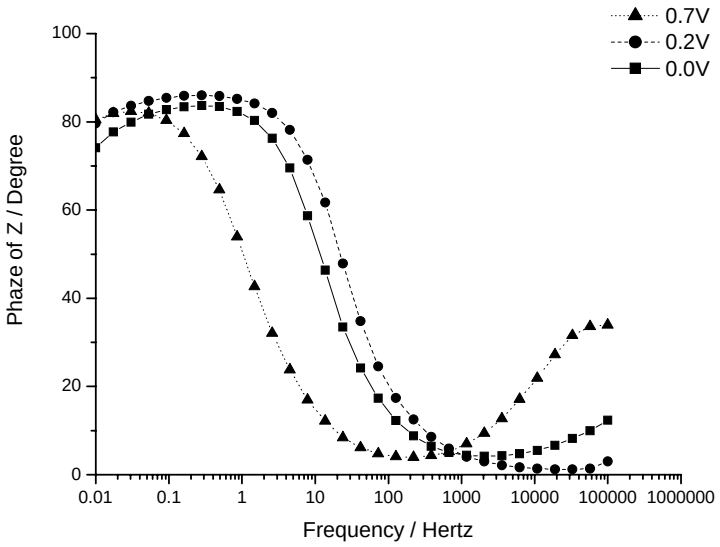

Figure A.8: Bode phase graph of PANI-CI grown applying 16 cycles.

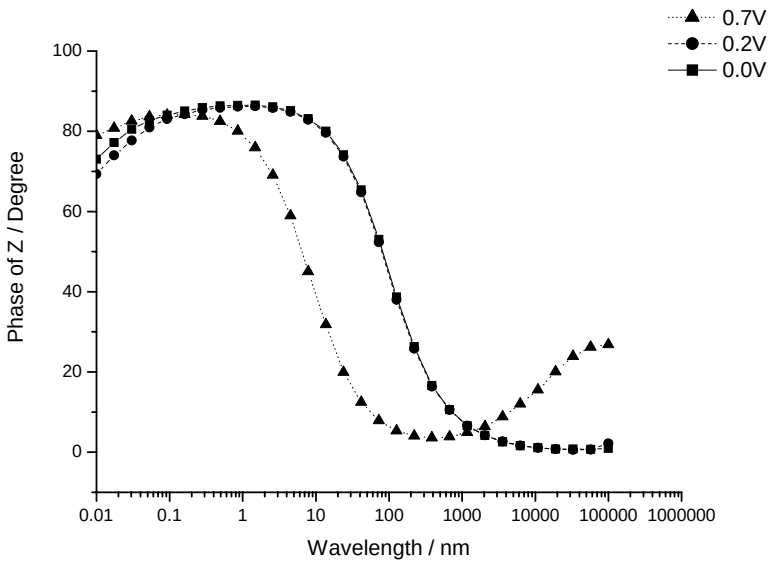

Figure A.9: Bode phase graph of PANIHCI-CI grown applying 16 cycles.

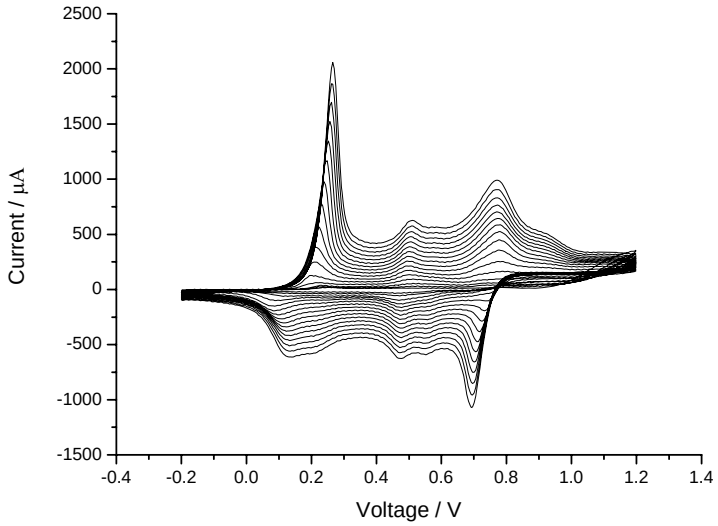

Figure A.10: The polymer growth of ANI in 1M MS at 100 mV/s scan rate applying 16 cycles.

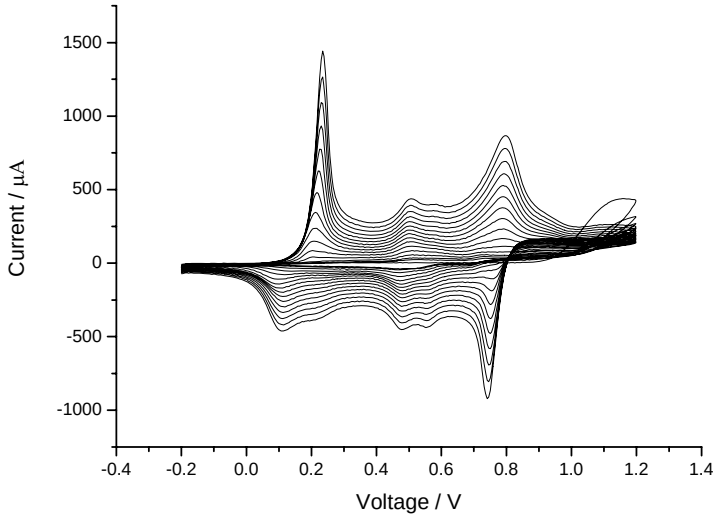

Figure A.11: The polymer growth of ANIMS in 1M MS at 100 mV/s scan rate applying 16 cycles.

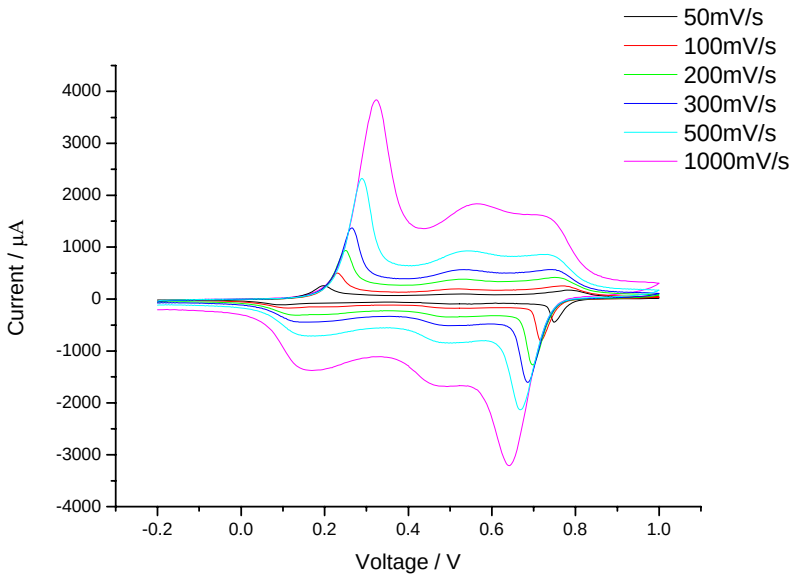

Figure A.12: Scan rate dependence of PANI-MS film (grown applying 8 cycles) in monomer free electrolyte at the different scan rates.

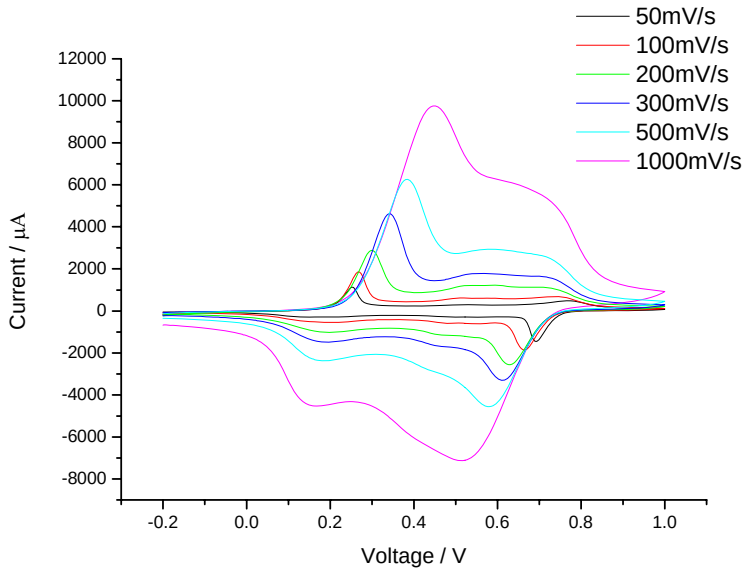

Figure A.13: Scan rate dependence of PANI-MS film (grown applying 16 cycles) in monomer free electrolyte at the different scan rates.

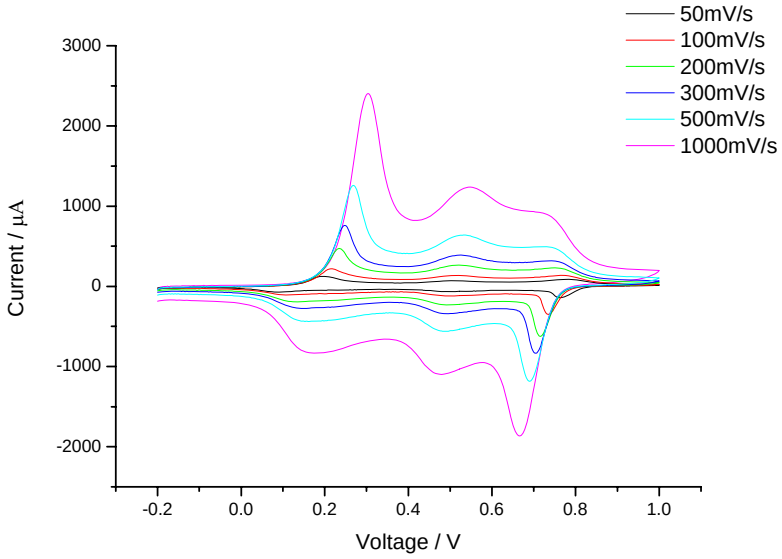

Figure A.14: Scan rate dependence of PANIMS-MS film (grown applying 8 cycles) in monomer free electrolyte at the different scan rates.

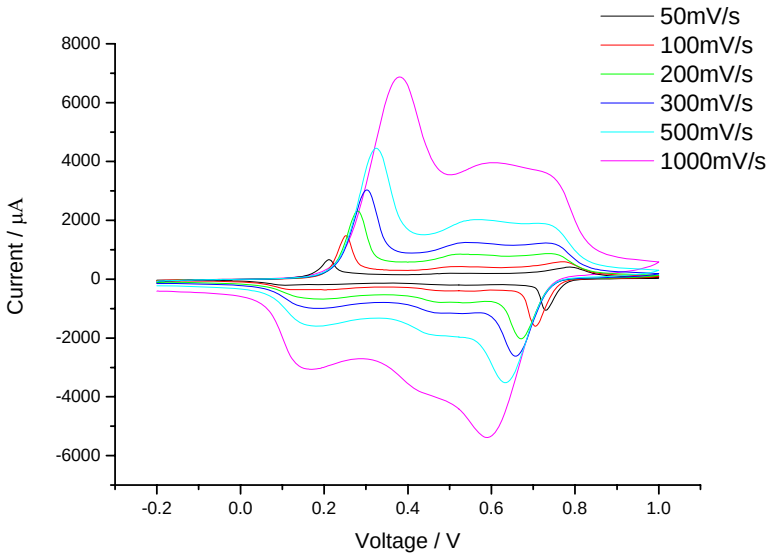

Figure A.15: Scan rate dependence of PANIMS-MS film (grown applying 16 cycles) in monomer free electrolyte at the different scan rates.

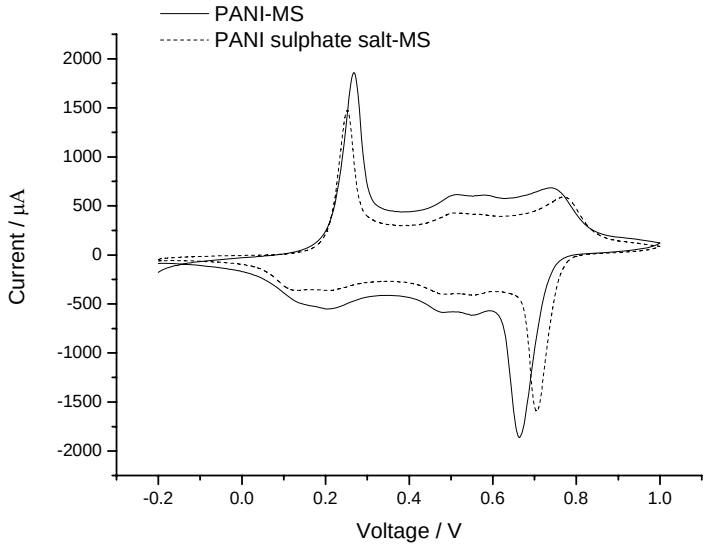

Figure A.16: The comparison of CV of PANI-MS and PANIMS -MS (grown applying 16 cycles) at the 100mV/s scan rate.

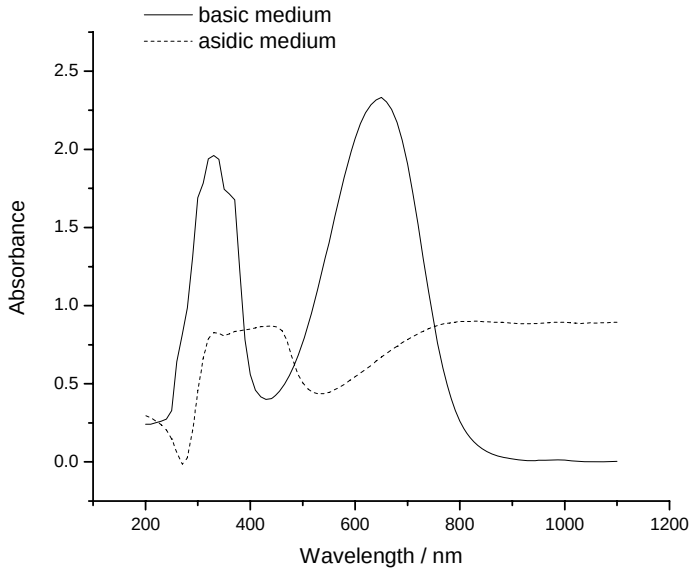

Figure A.17: UV-visible spectra of PANI-MS sample in the basic and acidic medium.

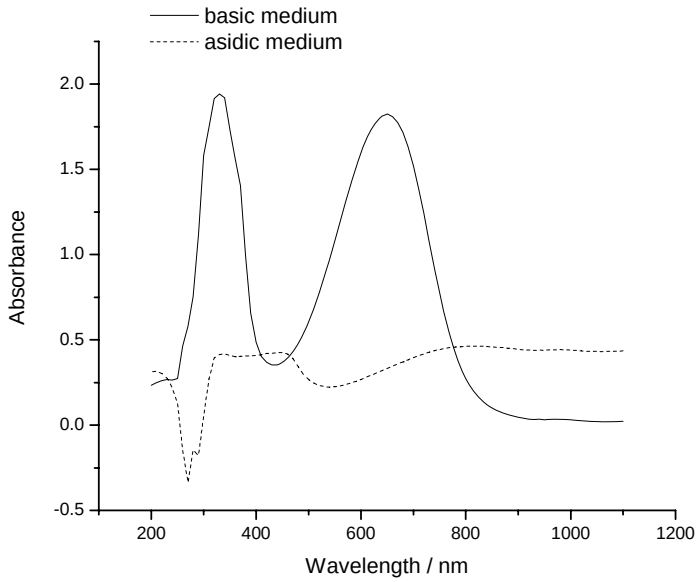

Figure A.18: UV-visible spectra of PANIMS-MS sample in the basic and acidic medium.

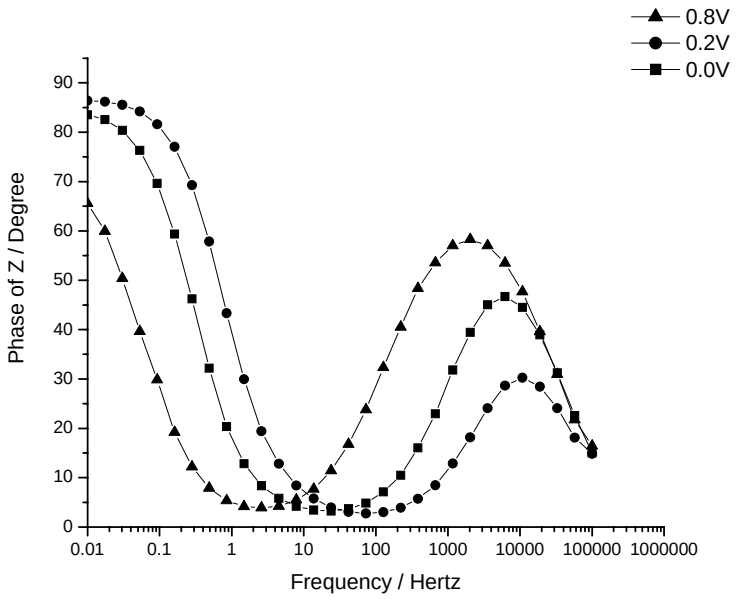

Figure A.19: Bode phase graph of PANI-MS grown applying 16 cycles.

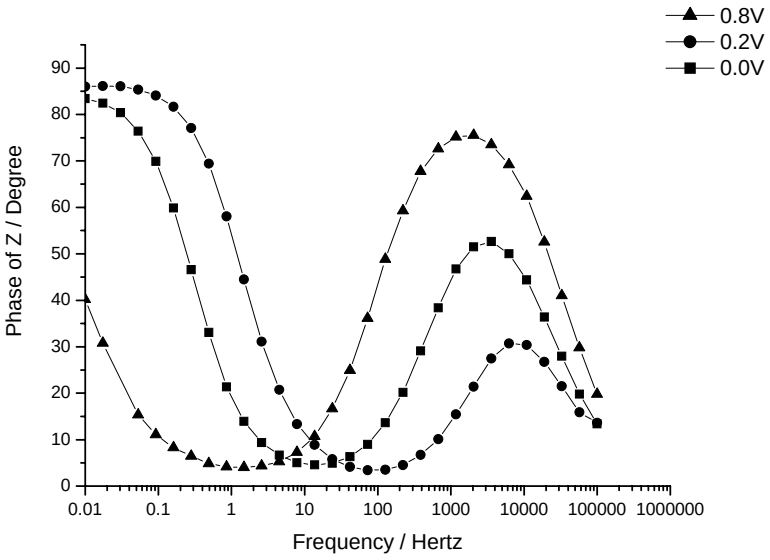

Figure A.20: Bode phase graph of PANIMS-MS grown applying 16 cycles.

RESUME

Dilek ÇAKIROĞLU was born in İskenderun in 1980. She admitted to Istanbul Technical University, Physics Engineering Department in 1997 and graduated as a Physics Engineer in 2003 fall term.

She was accepted as a M.Sc. student to the Polymer Science and Technology Programme of the Institute of Science and Technology of Istanbul Technical University in 2004.